© 2007 The Chemical Society of Japan

Award Accounts

The Chemical Society of Japan Award for Creative Work for 2005

Creation of Fullerene-Based Artificial Photosynthetic Systems

Hiroshi Imahori

Department of Molecular Engineering, Graduate School of Engineering, Kyoto University, Nishikyo-ku, Kyoto 615-8510

Fukui Institute for Fundamental Chemistry, Kyoto University, 34-4 Takano-Nishihiraki-cho, Sakyo-ku, Kyoto 606-8103

Received August 28, 2006; E-mail: imahori@scl.kyoto-u.ac.jp

Various porphyrin–fullerene-linked systems have been prepared to elucidate the intrinsic electron-transfer properties of fullerenes. Photodynamical studies on porphyrin–fullerene-linked systems showed that spherical fullerenes accelerated photoinduced electron transfer and charge-shift, but slowed down charge recombination, which is in sharp contrast with those of conventional planar acceptors such as quinones and imides. For the first time, it was shown that the unique electron-transfer properties result from the small reorganization energies of fullerenes arising from the delocalized π system on the sphere together with the rigid structure. The small reorganization energies make it possible to produce a long-lived charge-separated state with a high quantum yield in donor–fullerene systems. The finding also will allow us to construct light energy conversion systems as well as artificial photosynthetic models. Highly efficient photoinduced energy and electron transfer were achieved on gold and ITO electrodes modified with self-assembled monolayers of the porphyrin–fullerene-linked systems. We also developed dye-sensitized bulk heterojunction solar cell possessing both characteristics of dye-sensitized and bulk heterojunction solar cells. These results showed the advantages of fullerenes as electron acceptors in artificial photosynthetic model, photonic molecular devices and machines, and organic molecular electronics including solar cells.

1. Introduction

Recently, much attention has been focused on donor (D)–acceptor (A) interaction to elucidate the basic mechanisms for electron transfer (ET) in chemistry and biology.[1] In particular, D–A-linked systems have been frequently prepared to address the problems.[1] The main reason for studying such D–A-linked systems is to eliminate complex factors arising from diffusion in solutions and to use the high energy of singlet excited state, of which the lifetime is usually too short to undergo intermolecular ET in solution. Basic information obtained from the studies on D–A-linked systems is also important for the development of artificial photosynthetic systems including photoactive molecular devices and machines, photocatalysts, and organic solar cells.[1–19] Since artificial photosynthesis is based on photosynthetic processes in nature, purple bacterial photosynthesis, which possesses one of the simplest photosystem among photosynthetic organisms, is discussed.[20,21] The photosynthetic core in purple bacteria involves light-harvesting in antenna complexes and multistep ET in reaction centers, both of which are embedded in a lipid bilayer membrane, for efficient conversion of light energy into chemical energy, i.e., adenosine triphosphate (ATP), as shown in Fig. 1. Namely, solar energy is collected by bacteriochlorophylls (Bchl) and carotenoids (Car) in the antenna complexes (LH1 and LH2).[20,21] Then, the captured energy is transferred to the dimer of Bchl molecules ($(Bchl)_2$) in the reaction center, generating its singlet excited state ($^1(Bchl)_2{}^*$) which lies about 1.4 eV above the ground state. Within ≈3 ps, an ET occurs from $^1(Bchl)_2{}^*$ to the bacteriopheophytin (Bphe) molecule located $R_{ee} \approx 9$ Å (edge-to-edge distance) via a two-step sequential mechanism or a one-step superexchange mechanism. The energy of $(Bchl)_2{}^{\bullet+}Bphe^{\bullet-}$ (≈1.2 eV) is lowered by ≈0.2 eV, which matches the reorganization energy (λ) of ET to optimize the forward ET process, but the charge recombination (CR) process lies deep within the Marcus inverted region, which suppresses the CR process (vide infra). In a subsequent charge-shift (CSH) step, an electron is transferred in ≈200 ps from $Bphe^{\bullet-}$ to the primary quinone (Q_A) with an R_{ee} value of ≈9 Å. This reaction yields a charge-separated state, $(Bchl)_2{}^{\bullet+}Q_A{}^{\bullet-}$, which lies only ≈0.6 eV above the ground state. This implies that as much as 0.8 eV is lost to obtain the charge-separated state. In a final isoenergetic step, an ET takes place from $Q_A{}^{\bullet-}$ to the secondary quinone (Q_B), with a time constant of ≈100 μs. The resulting final charge-separated state with a lifetime of ≈1 s across the membrane eventually leads to the production of chemical energy. Note that the quantum efficiency for the production of $(Bchl)_2{}^{\bullet+}Q_B{}^{\bullet-}$ is ≈100%.[20,21] Purple bacteria use the energy of the reduced quinone (Q) to power a transmembrane hydrogen ion pump. A

Published on the web April 13, 2007; doi:10.1246/bcsj.80.621

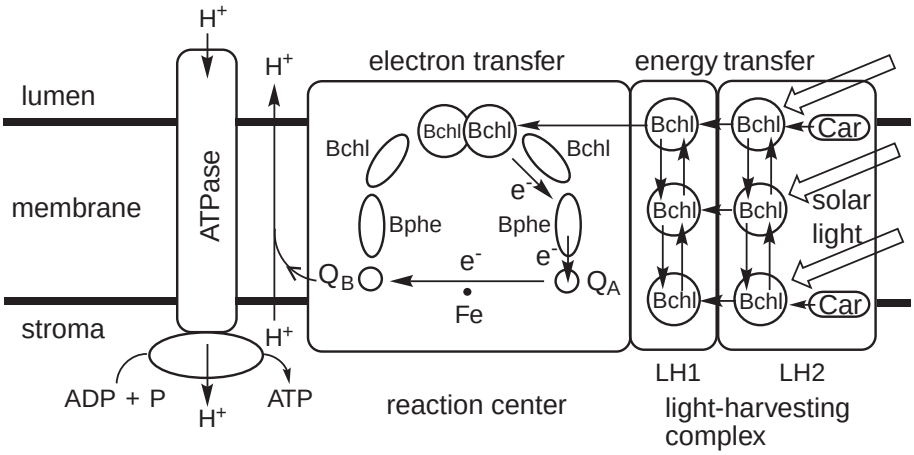

Fig. 1. Schematic view for conversion of solar energy into chemical energy in purple bacteria.

proton concentration gradient is generated across the membrane using cytochrome bc_1 complex. The proton gradient is further employed to convert adenosine diphosphate (ADP) to energy-rich ATP by ATP synthase (ATPase).[20,21]

2. Photosynthetic Electron Transfer in Porphyrin–Fullerene-Linked Systems

2.1 Multistep Electron Transfer and Small Reorganization Energy. Multistep ET is a key strategy in photosynthetic reaction centers. Although such multistep ET results in a substantial loss of input energy during each ET step, the resulting distantly separated radical ion pair attenuates the electronic coupling remarkably, thereby prolonging the lifetime of the final charge-separated state. To mimic such a multistep ET process in synthetic D–A systems, at least three components must be covalently linked to cause sequential ET within the molecule. Namely, the initial photoinduced ET from the sensitizer excited singlet state ($^1S^*$) to acceptor must be followed by subsequent ET from the A_1 radical anion ($A_1^{\bullet-}$) to A_2 or from D to the S radical cation ($S^{\bullet+}$). Thus, there are two types of sequential ET in the three component systems: S–A_1–A_2 and D–S–A (Fig. 2). Sakata, Mataga, et al. have reported the first synthesis and photophysical properties of the S–A_1–A_2 system consisting of a porphyrin (S) tethered to two quinones (A_1 and A_2).[22–24] The energy level of each state in the triad is designed in the order of $^1S^*$–A_1–A_2 > $S^{\bullet+}$–$A_1^{\bullet-}$–A_2 > $S^{\bullet+}$–A_1–$A_2^{\bullet-}$. Therefore, if the second ET from $A_1^{\bullet-}$ to A_2 can compete with the energy-wasting CR to the ground state, the final state $S^{\bullet+}$–A_1–$A_2^{\bullet-}$ will be produced in a total sequence of $^1S^*$–A_1–A_2 → $S^{\bullet+}$–$A_1^{\bullet-}$–A_2 → $S^{\bullet+}$–A_1–$A_2^{\bullet-}$. The well-separated charges slow down CR, as observed in the primary process in photosynthesis. Actually, the lifetime of $S^{\bullet+}$–A_1–$A_2^{\bullet-}$, produced via the sequential ET, has been found to be long considerably relative to that of the S–A_1 reference dyad.[22–24] This demonstrates the importance of multistep ET in a photosynthetic reaction center for prolonging the lifetime. Since the first demonstration of photosynthetic multistep ET,[22–24] a number of reports have been published dealing with the synthesis and photophysical properties of triads and more complex systems.[1–19] Some of these artificial photosynthetic reaction center models have exhibited the formation of a long-lived charge separated state with a high quantum yield, which is essential

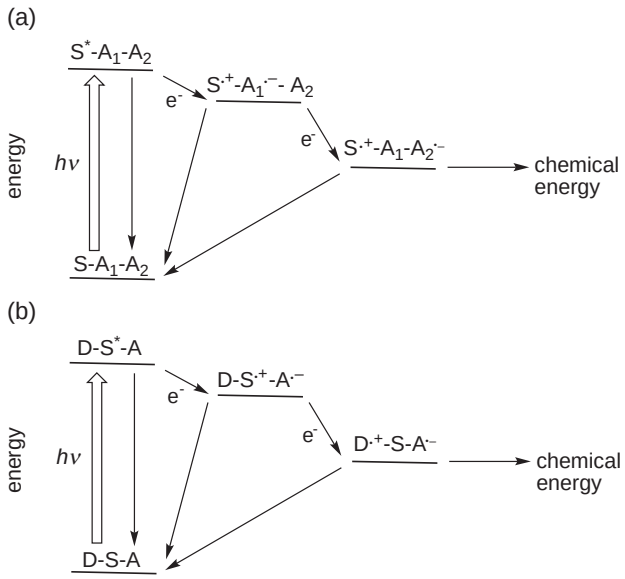

Fig. 2. Reaction pathways for (a) S–A_1–A_2 triad and (b) D–S–A triad mimicking photoinduced multistep ET in photosynthesis.

for efficient solar energy conversion. In particular, Gust, Moore, et al. have extensively developed a D–S–A type, i.e., carotenoid (D)–porphyrin (S)–quinone (A).[3,13,25] For instance, a sequential ET takes place from the porphyrin excited singlet state to the quinone, followed by a CSH from the carotenoid to the porphyrin radical cation, generating the final charge-separated state $D^{\bullet+}$–S–$A^{\bullet-}$ efficiently.[3,13,25] The advantage of Gust and Moore's system over Sakata and Mataga's system is the relatively rigid extended structure of the carotenoid–porphyrin–quinone triad which inhibits CR significantly, leading to the production of the relatively long-lived charge-separated state.

However, these model systems have lacked substantial methodology to optimize each ET process. It is essential to achieve fast forward ET and slow back ET for mimicking photosynthetic ET. In each ET process of natural reaction centers, forward ET is regulated to be much faster than back ET, resulting in the production of second lasting, long-lived final charge-separated state with an almost 100% quantum yield. λ has a

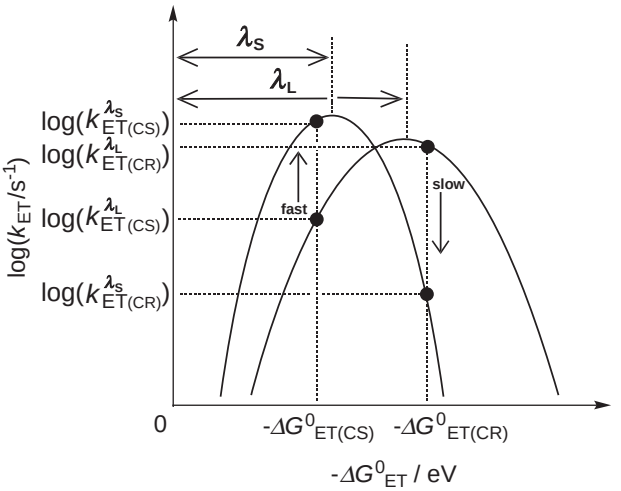

Fig. 3. Marcus parabolic curves for ET in two different D–A systems with small λ_S and large λ_L.

strong impact on the lifetime and quantum yield, and it is associated with change in the surrounding environment and molecular structures of D and A via ET. Since λ is one of the most important, albeit somewhat elusive, terms, first, we will briefly describe classical Marcus theory of ET,[26–28] which provides valuable guide for controlling and optimizing the efficiency of forward ET versus back ET. To quantify the driving force dependence on the ET rate constants (k_{ET}), Equation 1 is employed, where V is the electronic coupling matrix element, k_B is the Boltzmann constant, h is the Planck constant, T is the absolute temperature, and ΔG^0_{ET} is the free energy change.[26–28]

$$k_{ET} = \left(\frac{4\pi^3}{h^2\lambda k_B T}\right)^{1/2} V^2 \exp\left[-\frac{(\Delta G^0_{ET} + \lambda)^2}{4\lambda k_B T}\right]. \quad (1)$$

A typical Marcus ET curve, which provides insight into the importance of λ, is shown in Fig. 3. As $-\Delta G^0_{ET}$ becomes more positive, k_{ET} increases (normal region) until it reaches a maximum point where $-\Delta G^0_{ET} = \lambda$ (top region). As $-\Delta G^0_{ET}$ becomes even more positive, k_{ET} decreases (inverted region). This parabolic relationship between k_{ET} vs $-\Delta G^0_{ET}$ allows us to achieve ideal situation in which forward ET process proceeds under optimal conditions, that is, near the top region of the Marcus parabola, while the highly exergonic and energy-wasting back ET process is shifted deeply into the inverted region. Consequently, the forward ET is remarkably faster than the back ET, leading to the formation of a charge-separated state with both high quantum yield and long lifetime. This is the strategy that natural photosynthesis adopts for photosynthetic ET (vide supra).

However, in typical D–A-linked systems, such as porphyrin–quinone, porphyrin–imide, and diporphyrins dyads, λ have been reported to be 0.8–1.2 eV,[29–32] which are much larger than those in the primary process of charge separation (CS) in the purple bacteria reaction centers. In such cases, forward ET is comparable to or even slower than back ET, leading to less efficient production of the charge-separated state and/or with the short lifetime.[29–32] Although λ can be reduced by lowering the solvent polarity, the change is generally insufficient for optimizing such CS process. Thus, many researchers have considered that fast forward ET and slow back ET are difficult to be achieved in artificial D–A-linked systems. To surmount the problem, a new strategy is needed to lower λ. Let us consider two overlapping Marcus curves, i.e., two ET systems, where λ values are different, but other ET parameters including $-\Delta G^0_{ET}$ and V are identical (Fig. 3). Since loss of the initial energy, accompanied by forward ET should be minimal, $-\Delta G^0_{ET}$ for the forward ET is much smaller than that for the back ET. In such a case the forward ET process is in the Marcus normal region, whereas the back ET process is in the Marcus inverted region. When the forward k_{ET} on the two parabolic curves are compared in the Marcus normal region, you can find fast forward ET with a small λ and slow one with the large λ. In contrast, when the back k_{ET} on the two parabolic curves are compared in the Marcus inverted region, you can also see slow back ET with the small λ and fast one with the large λ. Therefore, a novel type of D and/or A exhibiting small λ is required to surmount the inevitable problem. In the following sections, we describe photoinduced accelerated forward ET and decelerated back ET in porphyrin–fullerene-linked systems and its application to photoelectrochemical devices and organic solar cells. We have successfully demonstrated that the unique ET properties of three-dimensional spherical fullerenes result from the small λ of fullerenes in comparison with those of conventional two-dimensional planar acceptors, such as quinones and diimides.[8,10,14–17]

2.2 Small Reorganization Energies of Fullerenes in Electron Transfer. Porphyrins are excellent electron donors as well as sensitizers, and the most frequently employed building blocks in artificial photosynthetic models.[1,33] In early 1990s, while my research group was exploring a novel type of acceptor, which can be covalently linked to porphyrin, fullerenes appeared as a new type of attractive electron acceptor.[34,35] As an example, C_{60} has the following basic characteristics: i) C_{60} consists solely of sixty carbon atoms and has a moderate size (diameter, 8.8 Å, estimated from CPK model) similar to those of benzoquinones (BQ) and naphthalene-1,8:4,5-bis(dicarboximides) (NIm) (8.6 Å), but three-dimensional round shape, ii) C_{60} has moderate electron-accepting abilities (−0.3– −0.4 V vs SCE) similar to those of BQ and NIm and reversibly accommodates up to six electrons, iii) energy levels of the first excited singlet (2.0 eV) and triplet states (1.6 eV) of C_{60} are comparable to those of porphyrins and are much lower than those of conventional planar acceptors including quinones and diimides (>2 eV), and iv) C_{60} has a rigid framework in the ground, excited and reduced states and high stability under severe conditions.[34,35] Some of these characteristics are in stark contrast to conventional acceptors, such as quinones and diimides. Thus, fullerenes should exhibit unique photophysical properties when they are convalently linked to porphyrins.

Photochemical and photophysical properties of fullerenes in polymer films[36–40] as well as in solutions[41–43] have been investigated by several groups. Photoinduced intermolecular ET from polymers to fullerenes in the films and from donors to fullerenes in solutions has been observed. Although occurrence of ultrafast photoinduced ET and metastability of the resulting charge-separated state at low temperature have been reported for the composite films,[37–40] the underlying ET properties of

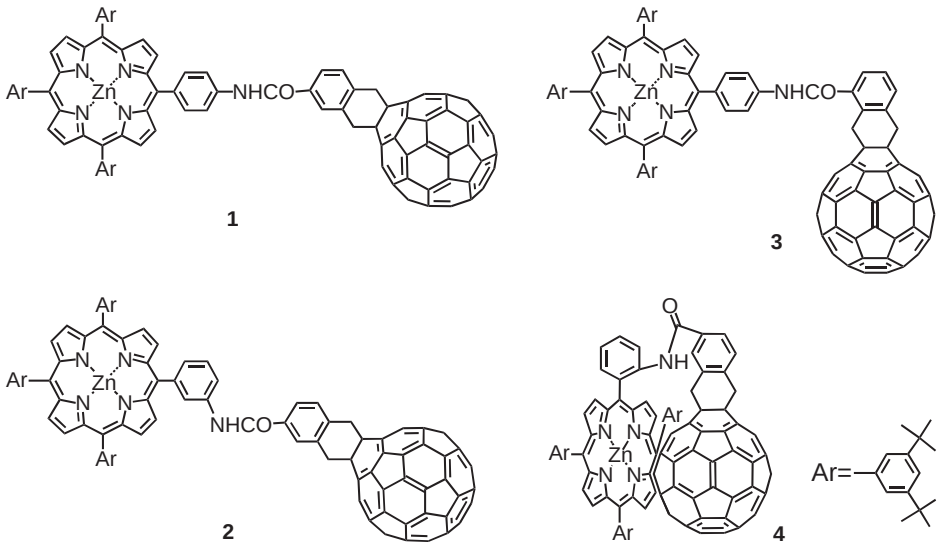

Fig. 4. ZnP–C_{60} dyads **1**–**4**.

fullerenes behind the interesting phenomenon have not been explored in the light of Marcus theory of ET. In this context, some of the first donor–C_{60}-linked dyads that were synthesized and studied photophysically to elucidate ET properties of fullerenes at the same time have been reported.[44–49] Gust, Moore, et al. have prepared porphyrin–fullerene-linked dyads,[44] and based on fluorescence lifetime measurements and energy level diagram, they have indicated that ET from the porphyrin excited singlet state to the C_{60} and/or from the porphyrin to the C_{60} excited singlet state is involved.[44] Verhoeven et al. have reported the synthesis and photophysical properties of aniline–C_{60}-linked dyad.[45] The fluorescence decay data show the occurrence of photoinduced ET from the aniline to the C_{60}. However, in both cases, they do not provide direct evidence for photoinduced ET in the dyads.[44,45] We prepared and studied porphyrinatozinc (ZnP)–C_{60}-linked dyads **1** (Fig. 4).[46–49] Six *tert*-butyl groups were introduced into *meso*-phenyl rings of the porphyrin moiety in **1** to increase the solubility in organic solvents. C_{60} was covalently tethered to a *meso*-porphyrin aryl ring at *para* position via amido bond at the final step of the synthesis to avoid tedious purification and characterization. It is interesting to note that condensation of 5-(4-aminophenyl)-10,15,20-triphenylporphyrin and C_{60} carboxylic acid under various conditions was unsuccessful probably due to the weak nucleophilicity of the amino group towards the carboxylic acid. Our photophysical studies regarding **1** using picosecond time-resolved transient absorption spectroscopy and fluorescence lifetime measurements offered the first direct experimental evidence for photoinduced intramolecular ET in donor-linked fullerenes.[46–49] After excitation of the ZnP moiety of **1**, transient absorption due to the porphyrin excited singlet state (^{1}ZnP*) appeared. As the absorption decayed, concomitant rise and decay of the transient bands due to porphyrinatozinc radical cation ($ZnP^{\bullet+}$) and C_{60} radical anion ($C_{60}^{\bullet-}$) were unambiguously detected, demonstrating photoinduced ET from the porphyrin excited singlet state to the C_{60} moiety in **1**. This pioneering work has been extended by our group to prepare a variety of porphyrin–C_{60}-linked systems.[49–96] At first, three additional porphyrinatozinc–C_{60}-linked dyads **2**–**4** were prepared by varying the linking position at *meso*-phenyl ring from *para* to *ortho* systematically.[49] Regardless of the linkage between the two chromophores, photoinduced CS and subsequent CR were observed in a series of porphyrinatozinc–C_{60}-linked dyads **1**–**4** by using picosecond fluorescence lifetime measurements and time-resolved transient absorption spectroscopy. It should be emphasized here that in the *ortho*-isomer **4** in which the C_{60} moiety is located closely on the porphyrin ring, we found specific π–π interaction between the porphyrin and the C_{60} based on the ^{1}H NMR spectrum, molecular modeling, and UV–visible absorption spectrum.[49] This finding has opened up the host–guest chemistry of porphyrins and fullerenes stemming from the specific π–π interaction.[97–100] Later, we found intra- and inter-molecular charge-transfer (CT) emission and absorption between porphyrins and fullerenes.[64,66,72,87,101] We determined various ET parameters, including V and λ, for porphyrin–fullerene systems from the CT absorption and emission for the first time.[64,66,72,87,101] Such CT absorption and emission were also reported for other fullerene–porphyrin-linked[102–105] and fullerene–phthalocyanine-linked[106] systems. Furthermore, the specific π–π interaction has been successfully used in dye-sensitized bulk heterojunction solar cells consisting of porphyrin and fullerene (vide infra).[107–118]

To compare the intrinsic ET properties of the three-dimensional spherical acceptors, i.e., fullerenes, vs the two-dimensional planar acceptors, i.e., quinones (Q), porphyrin–BQ-linked dyad **5** was synthesized (Fig. 5).[51] The first reduction potentials of the BQ (−0.45 V vs Ag/AgCl) and the C_{60} (−0.59 V vs Ag/AgCl) are largely similar. Furthermore, the

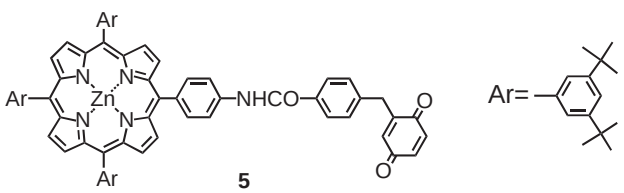

Fig. 5. ZnP–BQ dyad **5**.

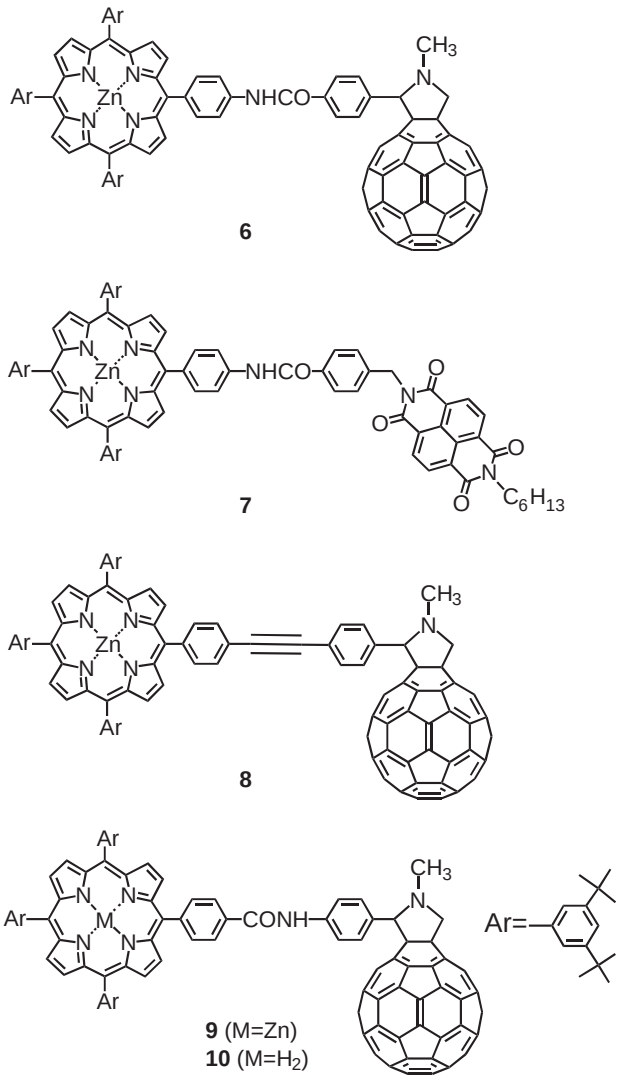

Fig. 6. ZnP–C_{60} dyads **6**, **8**, and **9**, H_2P–C_{60} dyad **10**, and P–NIm dyad **7**.

virtually same spacers between porphyrin and C_{60} or BQ ensures that the V values are almost identical. The forward electron transfer rate ($k_{ET(CS)}$) of **1** was found to be larger than that of **5**, whereas the charge-recombination rate ($k_{ET(CR)}$) of **1** is smaller than that of **5**.[51] A similar trend has been noted for porphyrin–fullerene dyad **6** and porphyrin–NIm dyad **7** with similar spacers (Fig. 6).[62,79] So far, a variety of donor–fullerene-linked systems have been prepared.[1,8–11,13–17,119–125] A fast photoinitiated $k_{ET(CS)}$ and relatively slow, dark $k_{ET(CR)}$ have been observed in many cases.[8–11,14–17,122,123] The ratios of $k_{ET(CS)}/k_{ET(CR)}$ in donor–C_{60}-linked dyads are much higher than those in conventional two-dimensional D–A dyads including porphyrin–quinones, porphyrin–diimides, and porphyrinatozinc–freebase porphyrins (H_2P).[29–32] Deceleration effect of higher fullerene, i.e., C_{70}, for CR was also observed for porphyrin–C_{70} dyad vs porphyrin–C_{60} dyad with the same spacer.[55,84] On the basis of the experimental results, we proposed, for the first time, that λ of fullerenes are much smaller than those of typical two-dimensional π acceptors.[51] The photoinduced CS process in the Marcus normal region becomes fast with decreasing the λ value, whereas the CR process in the Marcus inverted region becomes slow with decreasing the λ value. Therefore, photoinduced ET is accelerated, whereas the back ET is decelerated (vide supra). Initially, this proposal was not accepted as a reasonable explanation for the unique ET properties of fullerenes. Verhoeven, Paddon-Row, et al. presented photophysical properties of tetraalkyl-*p*-phenylenediamine-bridge–C_{60} dyad with a center-to-center distance (R_{cc}) of 18 Å between D and A.[126,127] They found similar fast photoinduced CS and slow CR for the dyad in benzonitrile. λ was estimated to be 1.2 eV in benzonitrile from the assumed vibrational λ ($\lambda_v = 0.3$ eV) and the Born-Hush approach with radii of D (3.7 Å) and A (5.6 Å). The estimated $-\Delta G^0_{ET}$ for photoinduced CS (0.44 eV) is much smaller than the λ (1.2 eV), but that for CR (1.29 eV) is comparable to the λ value. Thus, they have strongly insisted that the unique ET properties of fullerenes are not explained by λ, but are rationalized by large V value for photoinduced CS and small one for CR due to the coupling of certain C_{60} π orbitals with the geminal σ bonds of the bridge in addition to that with the vicinal σ bonds of the bridge stemming from the special symmetry properties of the C_{60} π-system.[126,127] Gust, Moore, and coworker have pointed out that the λ or the V may be responsible for the C_{60} effect.[128]

Our proposal is qualitatively explained by the large π-electron delocalization of C_{60} together with the rigid structure. λ is a sum of solvent (or outer sphere) term (λ_s) and λ_v (or inner sphere).[26–28] The unit charge in $C_{60}^{\bullet-}$ is delocalized over the three-dimensional carbon framework of C_{60}, while the charge in $BQ^{\bullet-}$ is localized largely on the two oxygen atoms. Furthermore, one side of the orbitals of the carbon atoms is buried inside the C_{60} sphere. Thus, taking into account the interaction between the charge and the surrounding solvent molecules, relevant charge density of each carbon in $C_{60}^{\bullet-}$ is much smaller than that of $BQ^{\bullet-}$, rendering λ_s of C_{60} small. The small Raman and Stokes shifts on reduction and photoexcitation of fullerenes support the rigid structure of C_{60}, where the λ_v is small.[129] Consequently, λ ($\lambda_s + \lambda_v$) of C_{60} would be smaller than that of BQ. Tachiya and Kato have predicted that λ for the sphere model is much smaller than that for the disk model.[130] In the sphere model, the surrounding solvent molecules are well separated from the center of the molecule, making the λ small. In the disk model, the surrounding solvent molecules, which are in contact with the top and the bottom of the disk, are close to the center of the molecule, making the λ large. A small λ_v of C_{60} (0.06 eV) has also been obtained from theoretical calculation.[131–133] In addition to the 1996 reports of the small λ of fullerenes, Guldi and Asmus have also reported relatively small λ values for C_{76} and C_{78} in intermolecular ET using pulse radiolysis.[134] The λ values of C_{76} and C_{78} (ca. 0.6 eV in CH_2Cl_2) are estimated on a CSH from the ground states of C_{76} and C_{78} to radical cation of various arenes, respectively. He has also suggested that the relatively small λ is beneficial for the possibility of establishing a Marcus inverted region. Later, we collaborated with Guldi to examine the driving force dependence of intermolecular ET reactions of fullerenes in details.[135] Pulse-radiolytic studies were performed to determine the rate constants of intermolecular ET from fullerenes (C_{60}, C_{76}, and C_{78}) to a series of arene radical cat-

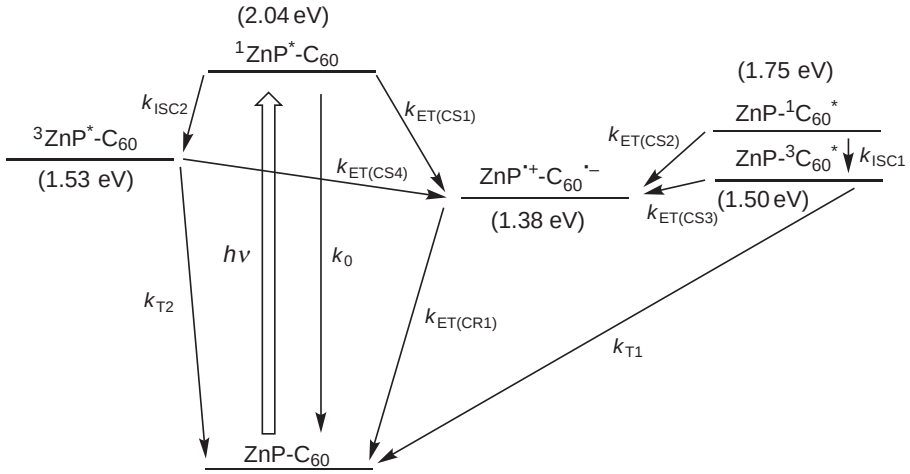

Scheme 1. Reaction scheme and energy diagram for **9** in benzonitrile.

ions in CH_2Cl_2. The redox potentials were measured electrochemically to determine an accurate $-\Delta G^0_{ET}$ value. We unambiguously confirmed the Marcus inverted region in both the ET reduction and oxidation of fullerenes. The average λ value for ET reduction of fullerenes was determined as 0.72 eV. The rather large λ value is similar to those for an intermolecular electron self-exchange reaction of tBuC$_{60}^-$/tBuC$_{60}^\bullet$ in benzonitrile/benzene (1/7 = v/v) (0.64 eV) and for BQ/BQ$^{\bullet-}$ couple in benzonitrile (0.74 eV).[133] In contrast, λ values ($\approx$0.3 eV) for an intermolecular electron self-exchange reaction of porphyrins and NIm in acetonitrile are much smaller than the λ value for fullerenes.[79] Intermolecular ET involving spherical three-dimensional fullerenes is likely to occur at large separation distances rendering the intermolecular λ large. In contrast, intermolecular ET between planar molecules is likely to take place at small separation distances due to π–π interaction, rendering the intermolecular λ small. Therefore, it is not appropriate to evaluate intrinsic λ in intermolecular ET systems. To compare intrinsic λ values of fullerenes and other acceptors, λ for intramolecular ET involving C_{60} and NIm were determined by using Marcus plot for $-\Delta G^0_{ET}$ vs k_{ET}.[79] The λ value of porphyrin–fullerene-linked dyads (0.59 eV for **6**, **8**, and **9**) is much smaller than that of porphyrin–NIm-linked dyad (1.41 eV for **7**), although the V values of the both systems are virtually the same. This is the first quantitative manifestation in which the λ value of a three-dimensional electron acceptor, i.e., C_{60}, is, indeed, much smaller than the value of a typical two-dimensional acceptor, i.e., NIm.[79]

We can also achieve a small reorganization energy in artificial systems when fullerenes are used as an electron acceptor. λ_s is a function of size, separation distance, and solvent polarity.[26–28] Thus, λ_s is expected to decrease with decreasing both the separation distance and the solvent polarity. Porphyrin–fullerene-linked dyad **4** and the freebase porphyrin (H_2P) analog are good candidates to minimize the λ value, because porphyrin and fullerene with small λ are fixed in a close proximity.[49,66,72] The values of ET parameters including λ, $-\Delta G^0_{ET}$, and V were determined by analyzing the CT absorption and emission in nonpolar solvents for the first time.[49,66,72] The λ of the freebase and zinc systems in benzene were estimated as 0.23 and 0.11 eV, which are the smallest values among inter- and intra-molecular D–A systems ever reported.[1–17] More importantly, they are comparable to the smallest values for the primary CS in the photosynthetic reaction centers.[20,21] Similar small λ have been obtained for intermolecular complexes between porphyrins and fullerenes in solid state[64] as well as other intramolecular systems.[104,106] The results clearly show that fullerenes combined with porphyrins are potential components for constructing artificial photosynthetic systems. The small λ values for porphyrin–fullerene systems are quite similar to those for photosynthetic reaction centers where efficient, long-lived CS is achieved by using multistep ET processes with tuning of λ to minimize the expenditure of $-\Delta G^0_{ET}$ and forcing the CR into the Marcus inverted region considerably. In such a case, the small λ value is attributed to the environmental effect of the surrounding protein residues. In contrast, planar porphyrin and spherical fullerene's delocalized π-electron systems with the rigid structures and high symmetries would make them possible to realize the intrinsic small λ of porphyrins and fullerenes, which would not be susceptible to the change of surrounding solvents or environments.

2.3 Photosynthetic Electron Transfer in Porphyrin–Fullerene-Linked Systems. We have prepared a variety of porphyrin–fullerene-linked systems to address the photodynamical properties.[46–96] Since such examples have been frequently described in our previous review articles,[8,10,14–17] we will present only a couple of the examples. First, as a representative example photodynamics of porphyrinatozinc–C_{60}-linked dyad **9** is presented.[63,65,68–70] Photoexcitation of **9** in polar solvents results in the occurrence of photoinduced ET, evolving all the excited states, that is, from ^{1}ZnP* and ^{3}ZnP* to C_{60} and from ZnP to ^{1}C$_{60}$* and ^{3}C$_{60}$*, creating the same charge-separated state, ZnP$^{\bullet+}$–C$_{60}^{\bullet-}$. The energy levels in benzonitrile are shown in Scheme 1 to illustrate the different relaxation pathways of photoexcited **9**. The total efficiency of ZnP$^{\bullet+}$–C$_{60}^{\bullet-}$ formation from the initial excited states in benzonitrile was estimated to be 99%. The resulting charge-separated state recombines to regenerate the ground state. $k_{ET(CR1)}$ was determined to be 1.3×10^6 s^{-1} from the decay kinetics of the C$_{60}^{\bullet-}$ fingerprint at 1000 nm in benzonitrile. Remarkably, this rate is nearly four orders of magnitude smaller than that for the fastest occurring CS from ^{1}ZnP* to C_{60} ($k_{ET(CS1)} = 9.5 \times 10^9$ s^{-1}). The

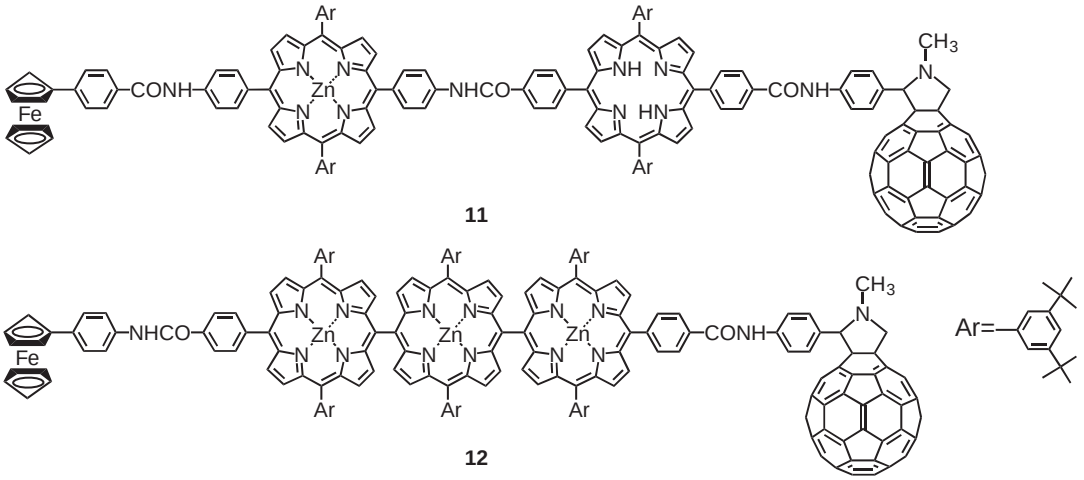

Fig. 7. Fc–ZnP–H_2P–C_{60} tetrad **11** and Fc–*meso*,*meso*-linked porphyrin trimer–C_{60} pentad **12**.

fast CS and slow CR of **9** in polar solvents are in stark contrast to conventional porphyrin–quinone- and porphyrin–diimide-linked dyads, where the $k_{ET(CR)}$ values are even larger than the $k_{ET(CS)}$ values in polar solvents. The $\log k_{ET}$ vs $-\Delta G^0_{ET}$ plots for **9** in polar solvents gave $\lambda = 0.66$ eV and $V = 3.9$ cm^{-1}.[69,70] It should be emphasized here that in **9** the CS processes from the singlet and triplet excited states of the C_{60} and from the singlet excited state of the porphyrin and the CR process are located in the normal, the top, and the inverted regions of the Marcus parabola, respectively. This unambiguously showed that a combination of porphyrin and fullerene is an ideal D–A couple for mimicking photosynthetic reaction center.

Systematic studies on the solvent dependent change in the CS and CR processes in **9** were performed.[65] Irrespective of the solvent polarity, photoinduced ET takes place from the porphyrin singlet excited state to the C_{60} moiety to produce a charge-separated state ($ZnP^{\bullet+}$–$C_{60}^{\bullet-}$). However, the resulting charge-separated state decays to different energy states depending on the energy level of the charge-separated state relative to those of the C_{60} singlet and triplet excited states. In nonpolar solvents, such as benzene ($\varepsilon_s = 2.28$), the charge-separated state undergoes CR to yield the C_{60} singlet excited state, followed by intersystem crossing to the C_{60} triplet excited state, since the energy level of the charge-separated state is higher than that of the C_{60} singlet excited state (1.75 eV) due to the destabilization of the charge-separated state in nonpolar solvents.[65] In more polar solvents, such as anisole ($\varepsilon_s = 4.33$), the energy level of the charge-separated state is located between those of the C_{60} singlet and triplet excited states.[65] As a result, photoinduced CS occurs from the porphyrin to the C_{60} singlet excited state as well as from the porphyrin singlet excited state to the C_{60}. In addition, the resulting charge-separated state decays to the C_{60} triplet excited state (1.50 eV) rather than the ground state. This CR to the triplet states is well-known in photosynthetic reaction centers.[20,21] In polar solvents, such as THF ($\varepsilon_s = 7.58$), benzonitrile ($\varepsilon_s = 25.2$), and DMF ($\varepsilon_s = 36.7$), the energy level of the charge-separated state (1.21–1.42 eV) is lower than those of the porphyrin (1.53 eV) and C_{60} triplet excited states (1.50 eV) (Scheme 1). Thus, all of the excited states lead to the production of the charge-separated state, which slowly decays to the ground state (vide supra). The solvent dependence of CR processes in **9** can be rationalized by small λ of porphyrins and fullerenes in ET processes.[65] A similar diagram can be drawn for the H_2P–C_{60} dyad **10** in polar solvents.[63,69,95] Photoinduced CS from the freebase porphyrin singlet excited state ($^1H_2P^*$ (1.89 eV)) to C_{60} in benzonitrile occurs to yield $H_2P^{\bullet+}$–$C_{60}^{\bullet-}$ (1.59 eV) with $k_{ET(CS1)}$ of 6.7×10^8 s^{-1} ($\Phi_{CS1}(^1H_2P^*) = 87\%$). In contrast to the porphyrinatozinc–C_{60} dyad **9**, the resulting charge-separated state decays with a rate constant of 5.0×10^7 s^{-1}, generating the porphyrin ($^3H_2P^*$) and fullerene ($^3C_{60}^*$) triplet states rather than the ground state, because the former processes are much faster than the latter process owing to the small λ of C_{60}. Photoinduced CS from the freebase porphyrin to the C_{60} excited singlet state (1.75 eV) may also occur to produce $H_2P^{\bullet+}$–$C_{60}^{\bullet-}$ (1.59 eV). Some fraction of H_2P–$^1C_{60}^*$ undergoes an intersystem crossing to yield H_2P–$^3C_{60}^*$ (1.50 eV), which then decays either to the ground state or to the $^3H_2P^*$–C_{60} state (1.40 eV).[69]

To prolong the lifetime of a final charge-separated state, we designed ferrocene (Fc)–ZnP–H_2P–C_{60} tetrad **11**,[70] as shown in Fig. 7. Each energy gradient was fine-tuned to mimic photosynthetic energy transfer (EN) and multistep ET processes (Scheme 2), leading to the formation of the final charge-separated state with well-separated charges. In addition, the utilization of C_{60} as an acceptor offers an advantage for acceleration of CS and deceleration of CR processes stemming from the small λ of C_{60} in ET. Thus, the lifetime of the final charge-separated state is expected to increase remarkably.

Picosecond transient spectroscopic measurements revealed that an efficient singlet–singlet EN ($k_{EN} \approx 3 \times 10^9$ s^{-1}) from ZnP to H_2P, governs the rapid deactivation of ^{1}ZnP* in **11**.[70] From $^1H_2P^*$, rapid intramolecular ET occurred with $k_{ET(CS1)} = 4.8 \times 10^9$ s^{-1} to yield Fc–ZnP–$H_2P^{\bullet+}$–$C_{60}^{\bullet-}$. The primary radical ion pair is then starting point to a cascade of short-range CSH reactions along the well-tuned redox gradient. This sequence eventually creates Fc^+–ZnP–H_2P–$C_{60}^{\bullet-}$, in which the charges are separated by $R_{ee} = 48.9$ Å. The total quantum yield of the CS in benzonitrile was moderate (24%) because of the significant contribution of undesirable deactivation pathways in Fc–ZnP–$H_2P^{\bullet+}$–$C_{60}^{\bullet-}$. Remarkably, intra-

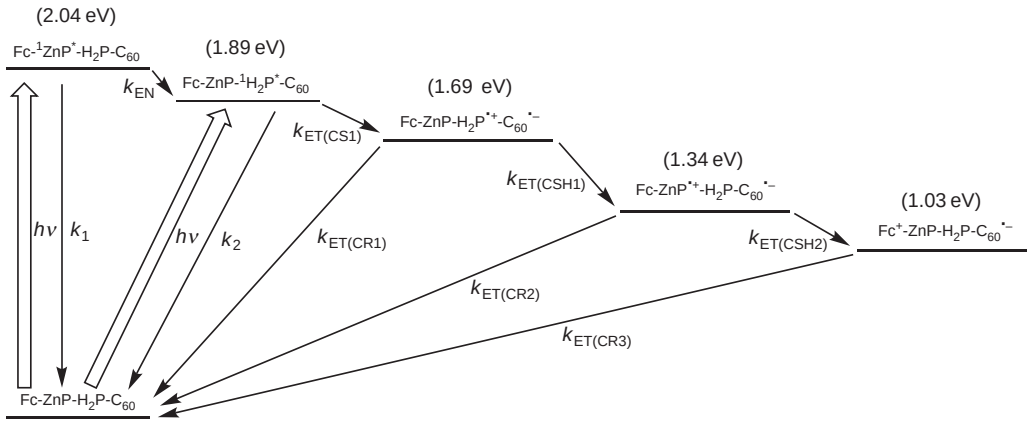

Scheme 2. Reaction scheme and energy diagram for **11** in benzonitrile.

molecular CR from $C_{60}^{•-}$ to Fc^+ was too slow to be observed in competition with the diffusion-limited intermolecular ET ($\approx 10^3\ s^{-1}$) from $C_{60}^{•-}$ in one tetrad to Fc^+ in another tetrad in a fluid solvent. In order to preclude the intermolecular ET against intramolecular ET processes in Fc^+–ZnP–H_2P–$C_{60}^{•-}$, electron spin resonance (ESR) measurements were performed in frozen polar solvents of **11** at various temperatures under illumination.[70] From the decay analysis of the final charge-separated state in benzonitrile at 163 K, the lifetime of the charge-separated state was found to be 0.38 s,[70] which was the longest value ever reported for intramolecular CR in D–A linked, multistep ET systems (see, previous examples; 200 μs in solutions[136] and 12.7 ms at 77 K[137]). Dependence of k_{ET} on the distance and driving force in a series of homologous porphyrin–fullerene-linked systems also validated the extremely long lifetime.[70] Further improvement of the longest lifetime of a final charge-separated state (1.6 s in DMF at 164 K) together with a total CS efficiency (34%) was recorded for Fc–ZnP–ZnP–C_{60} tetrad, in which the H_2P moiety of **11** was replaced by ZnP.[90]

Although the lifetimes of the final charge-separated states[70,90] are comparable to those of bacteriochlorophyll dimer radical cation ($(Bchl)_2^{•+}$)-secondary quinone radical anion ($Q_B^{•-}$) ion pair in bacteria photosynthetic reaction centers,[20,21] the maximal CS efficiency (34%) is still lower than the natural value (≈100%) in bacteria photosynthetic reaction centers. To improve a quantum yield for the formation of a final charge-separated state, we focused on *meso*,*meso*-linked porphyrins[18] as an excellent electron carrier as well as a light-harvesting antenna.[76,91] Namely, *meso*,*meso*-linked porphyrin trimer $(ZnP)_3$ as a light-harvesting chromophore was incorporated into photosynthetic multistep ET models including Fc as an electron donor and C_{60} as an electron acceptor to construct Fc–*meso*,*meso*-linked porphyrin trimer–fullerene pentad Fc–$(ZnP)_3$–C_{60} **12**[91] (Fig. 7). Photoexcitation of Fc–$(ZnP)_3$–C_{60} in polar solvents leads to the initial formation of Fc–$(ZnP)_3^{•+}$–$C_{60}^{•-}$ via photoinduced ET, followed by a CSH from Fc to $(ZnP)_3^{•+}$, to generate Fc^+–$(ZnP)_3$–$C_{60}^{•-}$.[91] The final charge-separated state in frozen DMF at 163 K decays obeying first-order kinetics with an extremely long lifetime of 0.53 s, as in the case of **11**. More importantly, the quantum yield for the formation of the final charge-separated state in **12** was found to be extremely high (83% in benzonitrile), despite of the large separation distance between the Fc^+ and $C_{60}^{•-}$ moieties ($R_{ee} = 46.9$ Å). The efficient CS through the porphyrin trimer is responsible for the high quantum yield, whereas the extremely slow CR is associated with the localized porphyrin radical cation in the middle porphyrin of the porphyrin trimer, which differs explicitly from the delocalized porphyrin radical cation in the porphyrin dimer.[76,91]

3. Self-Assembled Monolayers of Porphyrin–Fullerene-Linked Systems on Electrodes

In the previous sections, porphyrins and fullerenes were found to be excellent building blocks in artificial photosynthetic models. That is, "artificial photosynthesis" can be realized in a single molecule where an energetic, long-lived charge-separated state is generated with a high quantum yield. However, considering efficient conversion of the resulting charge-separated state into electrical or chemical energies, it is essential to arrange porphyrin–fullerene-linked molecules unidirectionally in organized media. Although Langmuir–Blodgett and lipid bilayer membranes have been frequently employed for the molecular organization,[138–146] instability and defects in the artificial membranes have limited successful development of the light energy conversion systems (internal quantum yield < 10%). We have focused on self-assembled monolayers (SAMs)[147,148] as a new methodology for molecular assembly. They enable the molecules of interest to be bound chemically on the surface such as metals, semiconductors, and insulators in a highly organized manner. Thus, they make it possible to arrange porphyrin–fullerene-linked molecules unidirectionally at the molecular level on substrates (i.e., electrodes) when substituents which self-assemble on the substrates are tethered to a terminal of the molecules.

Various SAMs of porphyrin–fullerene-linked systems have been prepared to mimic photosynthetic ET on electrodes.[52,56,59,61,67,77,78,86,92] In particular, alkanethiol has been tethered at the end of Fc–porphyrin (P)–C_{60} triads **13** (M = Zn) and **14** (M = H_2), because they can exhibit efficient formation of a final charge-separated state with a moderate lifetime via photoinduced multistep ET in solutions (Fig. 8).[58,59,61,67]

The photoelectrochemical experiments using the triad-modified gold electrode, a platinum wire and a Ag/AgCl electrode (denoted as Au/**13** or **14**/MV^{2+}/Pt device, where / de-

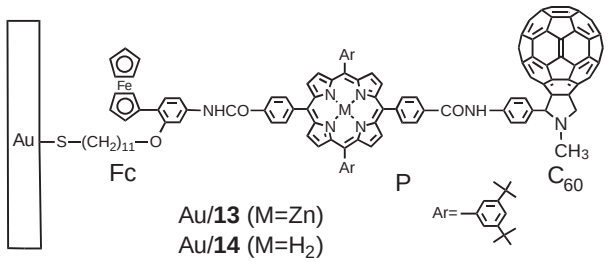

Fig. 8. SAMs of Fc–ZnP–C_{60} triad **13** (Au/**13**) and Fc–H_2P–C_{60} triad **14** (Au/**14**) on a gold electrode.

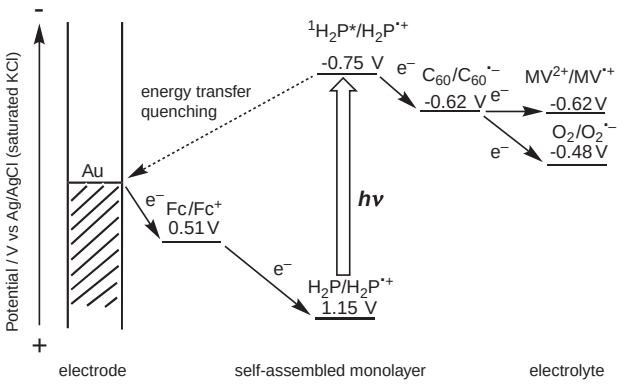

Scheme 3. Energy diagram for photocurrent generation on a gold electrode modified with self-assembled monolayer of **14**.

notes an interface) were performed in the presence of electron carriers, i.e., oxygen and methyl viologen (MV^{2+}). The internal quantum yields of cathodic photocurrent generation in Au/**13**/MV^{2+}/Pt and Au/**14**/MV^{2+}/Pt devices reached up to 20 and 25%, respectively.[61] The internal quantum yields are among the highest values of D–A-linked molecules on SAM-modified metal and ITO electrodes.[149–172] The high quantum yield is attained via photoinduced ET from the porphyrin singlet excited state to the C_{60} moiety, followed by the CSH from the Fc to the resulting porphyrin radical cation to produce the charge-separated state, Fc^+–P–$C_{60}^{\bullet-}$ in the monolayer (Scheme 3). Rapid ET to C_{60} due to the small λ can compete with the undesirable EN quenching by the gold electrode. Electron carriers, such as oxygen ($E^0_{red} = -0.48$ V for $O_2/O_2^{\bullet-}$) and/or MV^{2+} ($E^0_{red} = -0.62$ V for $MV^{+2}/MV^{\bullet+}$) are reduced by the $C_{60}^{\bullet-}$ moiety of Fc^+–P–$C_{60}^{\bullet-}$ to produce the reduced state which eventually give an electron to the counter electrode. On the other hand, k_{ET} from the gold electrode to Fc^+ in Fc^+–P–$C_{60}^{\bullet-}$ is controlled by the potential applied to the gold electrode. Thus, k_{ET} from the gold electrode to Fc^+ is increased with decreasing the applied potential, leading to an increase in the photocurrent.[61]

We have successfully constructed artificial reaction center on the gold electrode using Fc–P–C_{60} triads to mimic photosynthetic ET.[61] To mimic both light-harvesting in antenna complexes and CS in reaction centers simultaneously, we have to combine the artificial reaction center with artificial antenna complex on a gold electrode, which exhibits efficient photocurrent generation. Boron–dipyrrin alkanethiol **15** (Fig. 9) was in-

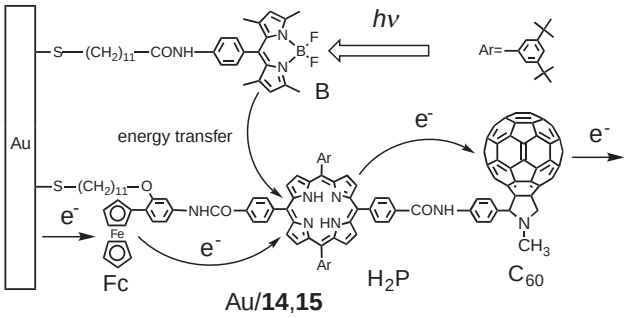

Fig. 9. Schematic view for photoinduced EN and multistep ET on a gold electrode modified with a mixed SAM of Fc–H_2P–C_{60} alkanethiol **14** and boron dipyrrin thiol **15** (Au/**14**,**15**).

corporated into Fc–H_2P–C_{60} triad (**14** in Fig. 8) on a gold electrode.[67] The incorporation allows us to enhance the absorption properties in the green region as well as the blue region. In addition, the emission from the boron–dipyrrin in **15** overlaps well with the absorption of the porphyrin moiety in **14**. Thus, efficient EN from the boron–dipyrrin moiety ($^1B^*$) in **15** to the porphyrin moiety (P) in **14** can take place in the mixed SAM of **14** and **15** on the gold electrode (Fig. 9). Overall, it is expected that boron–dipyrrin SAM combined with Fc–H_2P–C_{60} triad SAM can lead to efficient photocurrent generation, in addition to mimic coupled photoinduced EN and multistep ET in photosynthesis.

The maximum internal quantum yields of cathodic photocurrent generation were determined to be $50 \pm 8\%$ at 510 nm and $20 \pm 3\%$ at 430 nm for Au/**14**,**15**/MV^{2+}/Pt device and $1.6 \pm 0.3\%$ at 510 nm for Au/**15**/MV^{2+}/Pt reference device.[67] It should be emphasized that the maximum internal quantum yield of Au/**14**,**15**/MV^{2+}/Pt device at 510 nm is about 30 times larger than that of Au/**15**/MV^{2+}/Pt device at 510 nm. The internal quantum yield of the Au/**14**,**15**/MV^{2+}/Pt device, determined based on the absorbed photons by the porphyrin at 430 nm and the boron–dipyrrin at 510 nm, increased with an increase in the content of **14** in the SAM. The EN efficiency from the excited singlet state of the boron dipyrrin in **15** to the porphyrin in **14** also appeared to increase with an increase in the content of **14** in the SAM to reach the maximum value at 510 nm and a molar ratio of **14**:**15** = 63:37. The internal quantum yield ($50 \pm 8\%$) at 510 nm is the highest value ever reported for photocurrent generation on SAM-modified metal and ITO electrodes.[149–172]

4. Dye-Sensitized Bulk Heterojunction Solar Cell

As described in Section **3**, we have successfully prepared a variety of photoelectrochemical SAM comprising porphyrin or fullerene or both, which show photoinduced multistep ET and EN on gold and ITO surfaces. In these systems, however, the incident photon to photocurrent efficiency (IPCE or external quantum yield), which is strongly correlated with the light-harvesting efficiency, has been limited to be low (up to 1–2%) by the poor light-harvesting efficiency of the porphyrin monolayers.[67] Furthermore, the internal quantum yield of photocurrent generation is not sufficient in comparison with solar cells. To overcome such problems, we have to consider the follow-

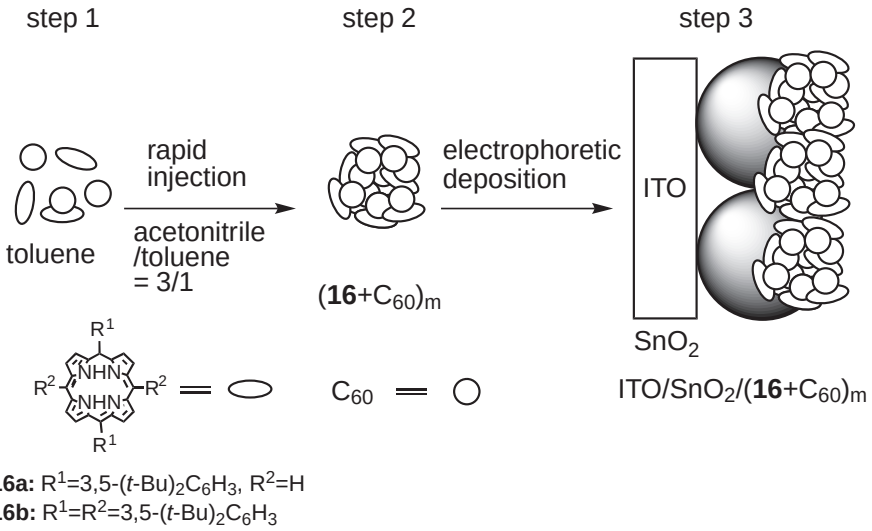

Scheme 4. Bottom-up self-organization of porphyrin and fullerene on a nanostructured SnO_2 electrode.

ing criteria: i) multilayer structures of porphyrin and fullerene on electrodes are prerequisite for improving the light-harvesting efficiency, ii) photoinduced CS efficiency between the interface of porphyrin and fullerene should be nearly 100%, iii) undesirable CR between the separated hole and electron should be minimized. As we mentioned before, porphyrin and fullerene make supramolecular complex due to the π–π interaction.[49,97–100] Such complexation will allow ultrafast CS in the complex, as in the case of bulk heterojunction solar cells.[173–194] In addition, undesirable CR will be suppressed by using suitable semiconducting electrode in which the separated electrons are injected into the conduction band (CB), as seen in dye-sensitized solar cells.[195–197] It should be noted here that, although porphyrin–fullerene-linked molecules are designed to exhibit long-lived charge-separated state with a high quantum yield in solutions, the linkage between D and A cannot be optimized for the desirable molecular packing of the dyads in the thin film on the electrode surface so that separated hole and electron do not undergo efficient hole and electron injection into the respective electrodes.

In a collaboration with Kamat et al., we applied step-by-step self-assembly to porphyrin and fullerene single components and the composites to construct a novel organic solar cell, dye-sensitized bulk heterojunction solar cell, possessing both the dye-sensitized and bulk heterojunction characteristics (Scheme 4).[16,17,107,118] First, supramolecular complex of porphyrin and fullerene is formed in toluene [denoted as (**16** + $C_{60})_m$] due to the π–π interaction (step 1). Then, the supramolecular complex is self-assembled into larger clusters in a mixture of toluene and acetonitrile due to lyophobic interaction between the complex and the mixed solvent (step 2). Finally, the larger clusters can be further associated onto a nanostructured SnO_2 electrode [denoted as ITO/SnO_2/(**16** + $C_{60})_m$] using the electrophoretic deposition technique[198] (step 3).

Photovoltaic properties of ITO/SnO_2/(**16a** + $C_{60})_m$ electrode were examined using acetonitrile containing NaI (0.5 M) (1 M = 1 mol dm^{-3}) and I_2 (0.01 M) as redox electrolyte and Pt gauge counter electrode [denoted as ITO/SnO_2/(**16a** + $C_{60})_m$/NaI + I_2/Pt device].[107] A short circuit photocurrent density (J_{SC}) of 0.18 mA cm^{-2}, open circuit voltage (V_{OC}) of 0.21 V, fill factor (*ff*) of 0.35, and η of 0.012% (input power (W_{IN}) = 110 mW cm^{-2}) were obtained for ITO/SnO_2/(**16a** + $C_{60})_m$/NaI + I_2/Pt device. The maximum IPCE value of 4.5% at 430 nm for ITO/SnO_2/(**16a** + $C_{60})_m$/NaI + I_2/Pt device is larger than the sum ($\approx$2%) of IPCE = 0.6% for ITO/SnO_2/(**16a**)$_m$/NaI + I_2/Pt and IPCE = 1.6% for ITO/SnO_2/$(C_{60})_m$/NaI + I_2/Pt reference devices. Note that a maximum IPCE value of 17% was obtained at 460 nm for ITO/SnO_2/(**16a** + $C_{60})_m$/NaI + I_2/Pt device at an applied potential of 0.2 V vs SCE. Such enhancement in the photocurrent generation of the composite cluster device from **16** and C_{60} demonstrates that CS between the excited porphyrin and C_{60} in the supramolecular complex is a dominating factor for efficient photocurrent generation. Namely, ultrafast photoinduced ET or CT occurs from the porphyrin singlet excited state ($^1H_2P^*/H_2P^{\bullet+}$ = −0.7 V vs NHE) to C_{60} ($C_{60}/C_{60}^{\bullet-}$ = −0.2 V vs NHE) in the complex. The reduced C_{60} injects electrons to the conduction band of SnO_2 nanocrystallites (E_{CB} = 0 V vs NHE) by electron hopping through large excess of C_{60} molecules, inhibiting CR. The regeneration of H_2P clusters ($H_2P/H_2P^{\bullet+}$ = 1.2 V vs NHE) is achieved by the iodide/triiodide couple (I^-/I_3^- = 0.5 V vs NHE) present in the electrolyte system (Scheme 5).[107]

The present organic solar cell, "dye-sensitized bulk heterojunction solar cell," is unique in that it possesses both characteristics of dye-sensitized and bulk heterojunction solar cells. Namely, initial CS takes place at the interface of D and A, which is typical characteristic of bulk heterojunction solar cells. Nevertheless, the following other processes are similar to those in dye-sensitized solar cells. It is noteworthy that the composite film has a multilayer structure on ITO/SnO_2, which presents a striking contrast to monolayer structure of adsorbed dyes on TiO_2 electrodes of dye-sensitized solar cells. Therefore, we can expect improvement of the photovoltaic properties by modulating both the structures of electrode surfaces and D–A multilayers.

We have extended the concept of dye-sensitized bulk heterojunction solar cells into more sophisticated supramolec-

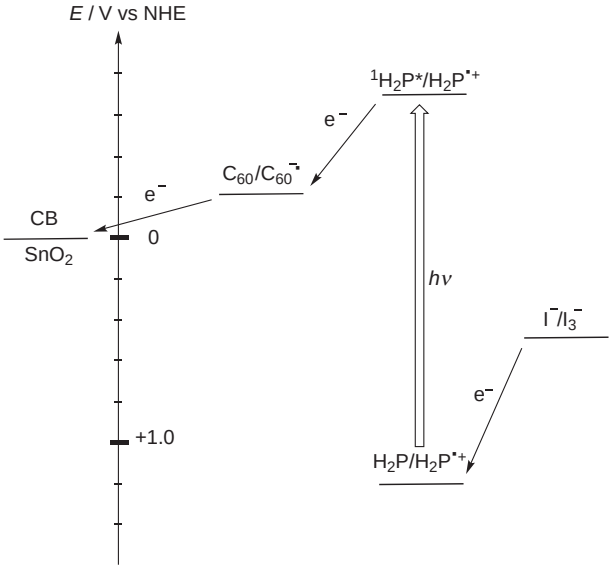

Scheme 5. Photocurrent generation diagram for dye-sensitized bulk heterojunction solar cell consisting of **16** and C_{60}.

ular systems prepared using bottom-up self-organization of porphyrin and fullerene with dendrimers[109,110] and nanoparticles[108,111–116] on a SnO_2 electrode. In particular, porphyrin–alkanethiol **17** (*n*: number of the methylene groups in the alkanethiol; $n = 5$, 11, and 15)[156] are three-dimensionally organized onto a gold nanoparticle with a diameter of ≈2 nm to give multiporphyrin-modified gold nanoparticles **18** ($n = 5$, 11, and 15)[199–202] with well-defined size (≈10 nm) and spherical shape (step 1 in Scheme 6). These nanoparticles bear flexible host space between the porphyrins for guest molecules, i.e., C_{60}. Thus, nanoparticles **18** incorporate C_{60} molecules between the porphyrin moieties due to π–π interaction (step 2), and the resultant supramolecular complexes grow into larger clusters with a size of ≈100 nm in the acetonitrile/toluene mixed solvent due to the lyophobic interaction (step 3). Finally, the large clusters are deposited electrophoretically onto the SnO_2 electrode (step 4). Photoelectrochemical measurements were performed with the standard two electrode system, denoted as ITO/SnO_2/(**18** + C_{60})$_m$/NaI + I_2/Pt device.[108,111] The IPCE value of ITO/SnO_2/(**18** + C_{60})$_m$/NaI + I_2/Pt device increased with an increase in the chain length ($n = 5$, 11, and 15) between the porphyrin and the gold nanoparticle. The longer methylene spacer of **18** allows suitable space for C_{60} molecules to accommodate them between the neighboring two porphyrin rings effectively compared to the clusters with the shorter methylene spacer, leading to more efficient photocurrent generation with up to IPCE value of 54% ($n = 15$). On the other hand, a further increase in the spacer length between the porphyrin and the gold nanoparticle results in a large decrease in the IPCE value.[115] Additionally, replacement of C_{60} with C_{70} or H_2P with ZnP leads to a decrease of the photoelectrochemical response.[111] The preference may be explained by the difference in the complexation abilities between the porphyrin and fullerene molecules as well as in the electron- or hole-hopping efficiency in the composite clusters. The ITO/SnO_2/(**18**($n = 15$) + C_{60})$_m$/NaI + I_2/Pt device has *ff* of

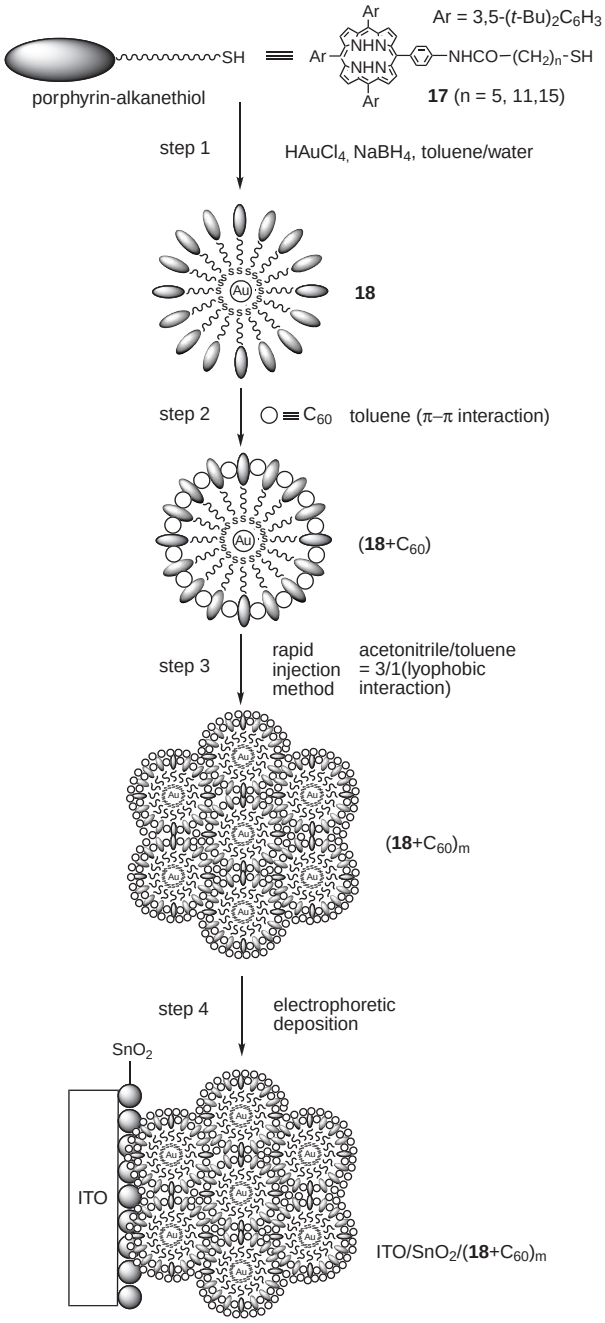

Scheme 6. Bottom-up self-organization of porphyrin and fullerene using gold nanoparticles on a nanostructured SnO_2 electrode.

0.43, V_{OC} of 0.38 V, J_{SC} of 1.0 mA cm^{-2}, and η of 1.5% at W_{IN} of 11.2 mW cm^{-2}. The *I*–*V* characteristics of ITO/SnO_2/(**18**($n = 15$) + C_{60})$_m$/NaI + I_2/Pt device is also remarkably enhanced by a factor of 45 in comparison with ITO/SnO_2/(**16b** + C_{60})$_m$/NaI + I_2/Pt reference device. These results clearly show that the large improvement of the photoelectrochemical properties results from three-dimensional interpenetrating network of the porphyrin and C_{60} molecules on the nanostructured SnO_2 electrode, which facilitates the injection of the separated electron into the conduction band.

The bottom-up self-assembled film of the composite clusters

exhibited IPCE value of up to 54%. However, preparation of such three-dimensionally pre-organized molecules is generally difficult and unlikely to be realistic for the future technological applications.[16,17,107–116,118,203,204] Therefore, it is highly desirable to exploit a supramolecular photoelectrochemical device consisting of simple, preprogrammed self-assembling porphyrin and C_{60} single component composites, which exhibit efficient photocurrent generation as a result of segregated nanoarrays of porphyrin and fullerene on SnO_2 electrodes.

We examined substituent effect of 5,10,15,20-tetraphenylporphyrin **19** on the nanostructure and photoelectrochemical properties of SnO_2 electrodes modified electrophoretically with the composite clusters of **19** and C_{60}.[117,118] To facilitate the surpramolecular complexation between the porphyrin and C_{60}, electron-donating substituents, i.e., methoxy group, were introduced at the 3,5-positions **19a**, 3,4,5-positions **19b**, and 2,6-positions **19c** of the *meso*-phenyl groups on the porphyrin ring. The maximum IPCE value (59% at 425 nm) of ITO/SnO_2/(**19a** + C_{60})$_m$ device was much larger than those of ITO/SnO_2/(**19b** + C_{60})$_m$ (10%), ITO/SnO_2/(**19c** + C_{60})$_m$ (5.7%), and other related porphyrin and C_{60} single component composite devices (1–17%).[107,117] It should be emphasized here that the simple substituent of methoxy groups onto the *meta*-positions of the *meso*-phenyl groups on the porphyrin ring is responsible for the efficient photocurrent generation, which is much superior to the systems from the more complex, time-consuming pre-organized porphyrin molecular assemblies and C_{60}.[107–116,203,204] Various spectroscopic and surface analyses showed that the molecular arrangement of **19a** and C_{60} composite clusters on the SnO_2 electrode was similar to the molecular packing in a single crystal of **19a**·2C_{60}·toluene. Porphyrin and C_{60} make an alternative layer structure, where the closest porphyrin moieties (R_{cc} = 14.2 Å) are arranged in a one-dimensional chain with a dihedral angle of 66°, while the closest C_{60} moieties (R_{cc} = 10.2 Å) in a two-dimensional sheet with sandwiching **19a** between two C_{60} molecules (Fig. 10).[117] The segregated nanoarrays of porphyrin and fullerene on the SnO_2 electrode allow the system to undergo ultrafast ET or CT (<100 fs) between the supramolecular complex of the porphyrin and C_{60} molecules, followed by hole and electron relay through the nanostructured one-dimensional porphyrin chains and two-dimensional C_{60} sheets, leading to the efficient photocurrent generation.[117] In bulk heterojunction solar cells many researchers have suggested the importance of nanostructured electron- and hole-transporting highways, which have never been confirmed experimentally.[173–194] Our finding provided the first evidence for the hypothesis. Such basic information will be valuable in the design of molecular photovoltaics in nanoscale.

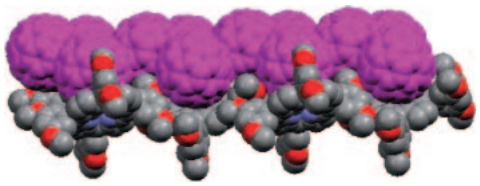

Fig. 10. Molecular packing of 5,10,15,20-tetrakis(3,5-dimethoxyphenyl)porphyrin (**19a**)·(C_{60})$_2$·(toluene). A part of C_{60} and toluene molecules are omitted for clarity.

5. Conclusion and Outlook

Porphyrins and fullerenes have been found to be an excellent building blocks by examining photoinduced intramolecular ET in the porphyrin–fullerene-linked systems using time-resolved spectroscopic methods covering from femtosecond to second time regions. The most remarkable characteristics of fullerenes in ET are that they accelerate photoinduced CS and to slow down CR. We proposed and demonstrated, for the first time, that the acceleration and deceleration effects of fullerenes arise from intrinsic small λ of fullerenes relative to those of conventional planar acceptors, i.e., quinone and diimide. The unique ET properties of fullerenes are associated with the three-dimensional delocalized π systems with spherical rigid, strained shape, and high symmetry. The elucidation of basic ET properties of fullerenes also provides us important basis for the high performance of fullerene-based organic molecular electronics including bulk heterojunction solar cells. Porphyrin–fullerene-linked systems display stepwise ET relay mimicking the primary CS in photosynthetic reaction centers. In particular, the lifetimes of final charge-separated state in the porphyrin–fullerene-linked tetrads and the pentad are the longest values ever reported for intramolecular CR in D–A-linked molecules based on multistep ET and are comparable to the lifetimes of bacteriochlorophyll dimer radical cation ($(Bchl)_2^{\bullet+}$)-secondary quinone radical anion ($Q_B^{\bullet-}$) ion pair in bacteria photosynthetic reaction centers. These results clearly show that fullerenes are good building blocks for the construction of artificial photosynthetic multicomponent systems.

We have applied porphyrin–fullerene-linked systems to SAMs on electrodes for the development of novel photoelectrochemical devices. The gold and ITO electrodes modified with porphyrin–fullerene-linked molecules have successfully mimicked photosynthetic EN and multistep ET. The internal quantum yield of the boron–dipyrrin and ferrocene–porphyrin–C_{60} triad system reaches up to 50%, which is the highest value among the previously reported artificial photosynthetic ET systems on the metal and ITO electrodes modified with SAMs.

Finally, we have successfully developed novel type of organic solar cell, dye-sensitized bulk heterojunction solar cell. In the solar cell, porphyrin and fullerene are assembled in a various manner onto nanostructured semiconducting electrodes which exhibit efficient photocurrent generation. Therefore, fullerene-based artificial photosynthetic systems are highly promising for the development of artificial photosynthetic models, photoactive molecular devices and machines, and organic molecular electronics including solar cells.

H. I. thanks Grants-in-Aid from MEXT, Japan (Priority Areas of Chemistry of Coordination Space (No. 18033025) and of Super-Hierarchical Structures (No. 18039019), and 21st Century COE on Kyoto University Alliance for Chemistry), NEDO, and Kurata and Sekisui foundations for financial support. H. I. is indebted to his colleagues and co-workers, particularly Yoshiteru Sakata, Shunichi Fukuzumi, Tadashi Okada, Iwao Yamazaki, Osamu Ito, Dirk. M. Guldi, Nikolai V. Tkachenko, Helge Lemmetyinen, Prashant V. Kamat, Hiroko Yamada, and Koichi Tamaki, for much of the work that is contained herein.

References

1 *Electron Transfer in Chemistry*, ed. by V. Balzani, WELEY-VCH, Weinheim, **2001**.
2 M. R. Wasielewski, *Chem. Rev.* **1992**, *92*, 435.
3 D. Gust, T. A. Moore, A. L. Moore, *Acc. Chem. Res.* **1993**, *26*, 198.
4 K. Maruyama, A. Osuka, N. Mataga, *Pure Appl. Chem.* **1994**, *66*, 867.
5 M. N. Paddon-Row, *Acc. Chem. Res.* **1994**, *27*, 18.
6 H. Kurreck, M. Huber, *Angew. Chem., Int. Ed. Engl.* **1995**, *34*, 849.
7 A. Harriman, J.-P. Sauvage, *Chem. Soc. Rev.* **1996**, *26*, 41.
8 H. Imahori, Y. Sakata, *Adv. Mater.* **1997**, *9*, 537.
9 J. W. Verhoeven, *Adv. Chem. Phys.* **1999**, *106*, 603.
10 H. Imahori, Y. Sakata, *Eur. J. Org. Chem.* **1999**, 2445.
11 D. M. Guldi, M. Prato, *Acc. Chem. Res.* **2000**, *33*, 695.
12 L. Sun, L. Hammarström, B. Åkermark, S. Styring, *Chem. Soc. Rev.* **2001**, *30*, 36.
13 D. Gust, T. A. Moore, A. L. Moore, *Acc. Chem. Res.* **2001**, *34*, 40.
14 H. Imahori, Y. Mori, Y. Matano, *J. Photochem. Photobiol., C* **2003**, *4*, 51.
15 H. Imahori, *Org. Biomol. Chem.* **2004**, *2*, 1425.
16 H. Imahori, S. Fukuzumi, *Adv. Funct. Mater.* **2004**, *14*, 525.
17 H. Imahori, *J. Phys. Chem. B* **2004**, *108*, 6130.
18 D. Kim, A. Osuka, *Acc. Chem. Res.* **2004**, *37*, 735.
19 M. R. Wasielewski, *J. Org. Chem.* **2006**, *71*, 5051.
20 *The Photosynthetic Reaction Center*, ed. by J. Deisenhofer, J. R. Norris, Academic Press, San Diego, **1993**.
21 *Anoxygenic Photosynthetic Bacteria*, ed. by R. E. Blankenship, M. T. Madigan, C. E. Bauer, Kluwer Academic Publishing, Dordrecht, **1995**.
22 M. Migita, T. Okada, N. Mataga, S. Nishitani, N. Kurata, Y. Sakata, S. Misumi, *Chem. Phys. Lett.* **1981**, *84*, 263.
23 S. Nishitani, N. Kurata, N. Nishimizu, Y. Sakata, S. Misumi, T. Okada, N. Mataga, 6th Symposium on Structural Organic Chemistry, Kyoto, **1982**, Abstr., No. B2-20.
24 S. Nishitani, N. Kurata, Y. Sakata, S. Misumi, A. Karen, T. Okada, N. Mataga, *J. Am. Chem. Soc.* **1983**, *105*, 7771.
25 T. A. Moore, D. Gust, P. Mathis, J. C. Mialocq, C. Chachaty, R. V. Bensasson, E. J. Land, D. Doizi, P. A. Liddell, G. A. Nemeth, A. L. Moore, *Nature* **1984**, *307*, 630.
26 R. A. Marcus, N. Sutin, *Biochim. Biophys. Acta* **1985**, *811*, 265.
27 R. A. Marcus, *Angew. Chem., Int. Ed. Engl.* **1993**, *32*, 1111.
28 M. Bixon, J. Jortner, *Adv. Chem. Phys.* **1999**, *106*, 35.
29 T. Asahi, M. Ohkohchi, R. Matsusaka, N. Mataga, R. P. Zhang, A. Osuka, K. Maruyama, *J. Am. Chem. Soc.* **1993**, *115*, 5665.
30 J. M. DeGraziano, P. A. Liddell, L. Leggett, A. L. Moore, T. A. Moore, D. Gust, *J. Phys. Chem.* **1994**, *98*, 1758.
31 A. Osuka, G. Noya, S. Taniguchi, T. Okada, Y. Nishimura, I. Yamazaki, N. Mataga, *Chem. Eur. J.* **2000**, *6*, 33.
32 A. Nakano, A. Osuka, T. Yamazaki, Y. Nishimura, S. Akimoto, I. Yamazaki, A. Itaya, M. Murakami, H. Miyasaka, *Chem. Eur. J.* **2001**, *7*, 3134.
33 *The Porphyrin Handbook*, ed. by K. M. Kadish, K. Smith, R. Guilard, Academic Press, San Diego, **2000**.
34 *Science of Fullerenes and Carbon Nanotubes*, ed. by M. S. Dresselhaus, G. Dresselhaus, P. C. Eklund, Academic Press, San Diego, **1996**.
35 *Fullerenes*, ed. by K. M. Kadish, R. S. Ruoff, John Wiley & Sons, New York, **2000**.
36 Y. Wang, *Nature* **1992**, *356*, 585.
37 N. S. Sariciftci, L. Smilowitz, A. Heeger, F. Wudl, *Science* **1992**, *258*, 1474.
38 S. Morita, A. A. Zakhidov, K. Yoshino, *Solid State Commun.* **1992**, *82*, 249.
39 M. Gevaert, P. V. Kamat, *J. Phys. Chem.* **1992**, *96*, 9883.
40 K. Lee, R. A. J. Janssen, N. S. Sariciftci, A. J. Heeger, *Phys. Rev. B* **1994**, *49*, 5781.
41 R. J. Sension, A. Z. Szarka, G. R. Smith, R. M. Hochstrasser, *Chem. Phys. Lett.* **1991**, *185*, 179.
42 P. V. Kamat, *J. Am. Chem. Soc.* **1991**, *113*, 9705.
43 J. W. Arbogast, C. S. Foote, M. Kao, *J. Am. Chem. Soc.* **1992**, *114*, 2277.
44 P. A. Liddell, J. P. Sumida, A. N. Macpherson, L. Noss, G. R. Seely, K. N. Clark, A. L. Moore, T. A. Moore, D. Gust, *Photochem. Photobiol.* **1994**, *60*, 537.
45 R. M. Williams, J. M. Zwier, J. W. Verhoeven, *J. Am. Chem. Soc.* **1995**, *117*, 4093.
46 H. Imahori, Y. Sakata, 7th Symposium on C_{60}, Nagoya, **1994**, Abstr., No. 200; K. Hagiwara, S. Taniguchi, M. Hasegawa, T. Okada, H. Imahori, Y. Sakata, Symposium on Photochemistry, Osaka, **1994**, Abstr., No. IA113.
47 H. Imahori, K. Hagiwara, T. Akiyama, S. Taniguchi, T. Okada, Y. Sakata, *Chem. Lett.* **1995**, 265.
48 H. Imahori, Y. Sakata, *Mem. Inst. Sci. Ind. Res., Osaka Univ.* **1995**, *52*, 69.
49 H. Imahori, K. Hagiwara, M. Aoki, T. Akiyama, S. Taniguchi, T. Okada, M. Shirakawa, Y. Sakata, *J. Am. Chem. Soc.* **1996**, *118*, 11771.
50 H. Imahori, Y. Sakata, *Chem. Lett.* **1996**, 199.
51 H. Imahori, K. Hagiwara, M. Aoki, T. Akiyama, S. Taniguchi, T. Okada, M. Shirakawa, Y. Sakata, *Chem. Phys. Lett.* **1996**, *263*, 545.
52 T. Akiyama, H. Imahori, A. Ajavakom, Y. Sakata, *Chem. Lett.* **1996**, 907.
53 H. Imahori, K. Yamada, M. Hasegawa, S. Taniguchi, T. Okada, Y. Sakata, *Angew. Chem., Int. Ed. Engl.* **1997**, *36*, 2626.
54 S. Higashida, H. Imahori, T. Kaneda, Y. Sakata, *Chem. Lett.* **1998**, 605.
55 K. Tamaki, H. Imahori, Y. Nishimura, I. Yamazaki, A. Shimomura, T. Okada, Y. Sakata, *Chem. Lett.* **1999**, 227.
56 H. Imahori, S. Ozawa, K. Ushida, M. Takahashi, T. Azuma, A. Ajavakom, T. Akiyama, M. Hasegawa, S. Taniguchi, T. Okada, Y. Sakata, *Bull. Chem. Soc. Jpn.* **1999**, *72*, 485.
57 K. Tamaki, H. Imahori, Y. Nishimura, I. Yamazaki, Y. Sakata, *Chem. Commun.* **1999**, 625.
58 M. Fujitsuka, O. Ito, H. Imahori, K. Yamada, H. Yamada, Y. Sakata, *Chem. Lett.* **1999**, 721.
59 H. Imahori, H. Yamada, S. Ozawa, K. Ushida, Y. Sakata, *Chem. Commun.* **1999**, 1165.
60 K. Yamada, H. Imahori, Y. Nishimura, I. Yamazaki, Y. Sakata, *Chem. Lett.* **1999**, 895.
61 H. Imahori, H. Yamada, Y. Nishimura, I. Yamazaki, Y. Sakata, *J. Phys. Chem. B* **2000**, *104*, 2099.
62 H. Imahori, K. Tamaki, H. Yamada, K. Yamada, Y. Sakata, Y. Nishimura, I. Yamazaki, M. Fujitsuka, O. Ito, *Carbon* **2000**, *38*, 1599.
63 C. Luo, D. M. Guldi, H. Imahori, K. Tamaki, Y. Sakata,

J. Am. Chem. Soc. **2000**, *122*, 6535.
64 N. V. Tkachenko, C. Guenther, H. Imahori, K. Tamaki, Y. Sakata, H. Lemmetyinen, S. Fukuzumi, *Chem. Phys. Lett.* **2000**, *326*, 344.
65 H. Imahori, M. E. El-Khouly, M. Fujitsuka, O. Ito, Y. Sakata, S. Fukuzumi, *J. Phys. Chem. A* **2001**, *105*, 325.
66 H. Imahori, N. V. Tkachenko, V. Vehmanen, K. Tamaki, H. Lemmetyinen, Y. Sakata, S. Fukuzumi, *J. Phys. Chem. A* **2001**, *105*, 1750.
67 H. Imahori, H. Norieda, H. Yamada, Y. Nishimura, I. Yamazaki, Y. Sakata, S. Fukuzumi, *J. Am. Chem. Soc.* **2001**, *123*, 100.
68 S. Fukuzumi, H. Imahori, H. Yamada, M. E. El-Khouly, M. Fujitsuka, O. Ito, D. M. Guldi, *J. Am. Chem. Soc.* **2001**, *123*, 2571.
69 H. Imahori, K. Tamaki, D. M. Guldi, C. Luo, M. Fujitsuka, O. Ito, Y. Sakata, S. Fukuzumi, *J. Am. Chem. Soc.* **2001**, *123*, 2607.
70 H. Imahori, D. M. Guldi, K. Tamaki, Y. Yoshida, C. Luo, Y. Sakata, S. Fukuzumi, *J. Am. Chem. Soc.* **2001**, *123*, 6617.
71 H. Imahori, T. Hasobe, H. Yamada, P. V. Kamat, S. Barazzouk, M. Fujitsuka, O. Ito, S. Fukuzumi, *Chem. Lett.* **2001**, 784.
72 V. Vehmanen, N. V. Tkachenko, H. Imahori, S. Fukuzumi, H. Lemmetyinen, *Spectrochim. Acta, Part A* **2001**, *57*, 2229.
73 S. Fukuzumi, K. Ohkubo, H. Imahori, J. Shao, Z. Ou, G. Zheng, Y. Chen, R. K. Pandey, M. Fujitsuka, O. Ito, K. M. Kadish, *J. Am. Chem. Soc.* **2001**, *123*, 10676.
74 H. Imahori, K. Tamaki, Y. Araki, T. Hasobe, O. Ito, A. Shimomura, S. Kundu, T. Okada, Y. Sakata, S. Fukuzumi, *J. Phys. Chem. A* **2002**, *106*, 2803.
75 S. Fukuzumi, H. Imahori, K. Okamoto, H. Yamada, M. Fujitsuka, O. Ito, D. M. Guldi, *J. Phys. Chem. A* **2002**, *106*, 1903.
76 H. Imahori, K. Tamaki, Y. Araki, Y. Sekiguchi, O. Ito, Y. Sakata, S. Fukuzumi, *J. Am. Chem. Soc.* **2002**, *124*, 5165.
77 H. Yamada, H. Imahori, Y. Nishimura, I. Yamazaki, S. Fukuzumi, *Adv. Mater.* **2002**, *14*, 892.
78 H. Yamada, H. Imahori, S. Fukuzumi, *J. Mater. Chem.* **2002**, *12*, 2034.
79 H. Imahori, H. Yamada, D. M. Guldi, Y. Endo, A. Shimomura, S. Kundu, K. Yamada, T. Okada, Y. Sakata, S. Fukuzumi, *Angew. Chem., Int. Ed.* **2002**, *41*, 2344.
80 T. J. Kesti, N. V. Tkachenko, V. Vehmanen, H. Yamada, H. Imahori, S. Fukuzumi, H. Lemmetyinen, *J. Am. Chem. Soc.* **2002**, *124*, 8067.
81 K. Ohkubo, H. Imahori, J. Shao, Z. Ou, K. M. Kadish, Y. Chen, G. Zheng, R. K. Pandey, M. Fujitsuka, O. Ito, S. Fukuzumi, *J. Phys. Chem. A* **2002**, *106*, 10991.
82 N. V. Tkachenko, V. Vehmanen, J.-P. Nikkanen, H. Yamada, H. Imahori, S. Fukuzumi, H. Lemmetyinen, *Chem. Phys. Lett.* **2002**, *366*, 245.
83 N. Ohta, S. Mikami, Y. Iwaki, M. Tsushima, H. Imahori, K. Tamaki, Y. Sakata, S. Fukuzumi, *Chem. Phys. Lett.* **2003**, *368*, 230.
84 T. Kesti, N. V. Tkachenko, H. Yamada, H. Imahori, S. Fukuzumi, H. Lemmetyinen, *Photochem. Photobiol. Sci.* **2003**, *2*, 251.
85 Y. Kashiwagi, K. Ohkubo, J. A. McDonald, I. M. Blake, M. J. Crossley, Y. Araki, O. Ito, H. Imahori, S. Fukuzumi, *Org. Lett.* **2003**, *5*, 2719.
86 H. Yamada, H. Imahori, Y. Nishimura, I. Yamazaki, T. K. Ahn, S. K. Kim, D. Kim, S. Fukuzumi, *J. Am. Chem. Soc.* **2003**, *125*, 9129.
87 N. V. Tkachenko, H. Lemmetyinen, J. Sonoda, K. Ohkubo, T. Sato, H. Imahori, S. Fukuzumi, *J. Phys. Chem. A* **2003**, *107*, 8834.
88 I. Zilbermann, G. A. Anderson, D. M. Guldi, H. Yamada, H. Imahori, S. Fukuzumi, *J. Porphyrins Phthalocyanines* **2003**, *7*, 357.
89 K. Ohkubo, H. Kotani, J. Shao, Z. Ou, K. M. Kadish, G. Li, R. K. Pandey, M. Fujitsuka, O. Ito, H. Imahori, S. Fukuzumi, *Angew. Chem., Int. Ed.* **2004**, *43*, 853.
90 D. M. Guldi, H. Imahori, K. Tamaki, Y. Kashiwagi, H. Yamada, Y. Sakata, S. Fukuzumi, *J. Phys. Chem. B* **2004**, *108*, 541.
91 H. Imahori, Y. Sekiguchi, Y. Kashiwagi, T. Sato, Y. Araki, O. Ito, H. Yamada, S. Fukuzumi, *Chem. Eur. J.* **2004**, *10*, 3184.
92 H. Imahori, M. Kimura, K. Hosomizu, T. Sato, T. K. Ahn, S. K. Kim, D. Kim, Y. Nishimura, I. Yamazaki, Y. Araki, O. Ito, S. Fukuzumi, *Chem. Eur. J.* **2004**, *10*, 5111.
93 T. Vuorinen, K. Kaunisto, N. V. Tkachenko, A. Efimov, A. S. Alekseev, K. Hosomizu, H. Imahori, H. Lemmetyinen, *Langmuir* **2005**, *21*, 5383.
94 V. Chukharev, T. Vuorinen, A. Efimov, N. V. Tkachenko, M. Kimura, S. Fukuzumi, H. Imahori, H. Lemmetyinen, *Langmuir* **2005**, *21*, 6385.
95 Y. Kobori, S. Yamauchi, K. Akiyama, S. Tero-Kubota, H. Imahori, S. Fukuzumi, J. R. Norris, *Proc. Natl. Acad. Sci. U.S.A.* **2005**, *102*, 10017.
96 M. Isosomppi, N. V. Tkachenko, A. Efimov, K. Kaunisto, K. Hosomizu, H. Imahori, H. Lemmetyinen, *J. Mater. Chem.* **2005**, *15*, 4546.
97 D. R. Evans, N. L. P. Fackler, Z. Xie, C. E. F. Rickard, P. D. W. Boyd, C. A. Reed, *J. Am. Chem. Soc.* **1999**, *121*, 8466.
98 M. M. Olmstead, D. A. Costa, K. Maitra, B. C. Noll, S. L. Phillips, P. M. Van Calcar, A. L. Balch, *J. Am. Chem. Soc.* **1999**, *121*, 7090.
99 K. Tashiro, T. Aida, J.-Y. Zheng, K. Kinbara, K. Saigo, S. Sakamoto, K. Yamaguchi, *J. Am. Chem. Soc.* **1999**, *121*, 9477.
100 P. D. W. Boyd, C. A. Reed, *Acc. Chem. Res.* **2005**, *38*, 235.
101 M. Wahadoszamen, T. Nakabayashi, S. Kang, H. Imahori, N. Ohta, *J. Phys. Chem. B* **2006**, *110*, 20354.
102 N. Armaroli, G. Marconi, L. Echegoyen, J. P. Bourgeois, F. Diederlich, *Chem. Eur. J.* **2000**, *6*, 1629.
103 D. Bonifazi, M. Scholl, F. Song, L. Echegoyen, G. Accorsi, N. Armaroli, F. Diederlich, *Angew. Chem., Int. Ed.* **2003**, *42*, 4966.
104 D. I. Schuster, P. Cheng, P. D. Jarowski, D. M. Guldi, C. Luo, L. Echegoyen, S. Pyo, A. R. Holzwarth, S. E. Braslavsky, R. M. Williams, G. Klihm, *J. Am. Chem. Soc.* **2004**, *126*, 7257.
105 N. Armaroli, G. Accorsi, F. Song, A. Palkar, L. Echegoyen, D. Bonifazi, F. Diederlich, *ChemPhysChem* **2005**, *6*, 732.
106 D. M. Guldi, I. Zilbermann, A. Gouloumis, P. Vazquez, T. Torres, *J. Phys. Chem. B* **2004**, *108*, 18485.
107 T. Hasobe, H. Imahori, S. Fukuzumi, P. V. Kamat, *J. Phys. Chem. B* **2003**, *107*, 12105.
108 T. Hasobe, H. Imahori, S. Fukuzumi, P. V. Kamat, *J. Am. Chem. Soc.* **2003**, *125*, 14962.
109 T. Hasobe, Y. Kashiwagi, M. Absalom, K. Hosomizu, M. J. Crossley, H. Imahori, P. V. Kamat, S. Fukuzumi, *Adv. Mater.* **2004**, *16*, 975.
110 T. Hasobe, P. V. Kamat, M. A. Absalom, Y. Kashiwagi, J. Sly, M. J. Crossley, K. Hosomizu, H. Imahori, S. Fukuzumi,

J. Phys. Chem. B **2004**, *108*, 12865.
111 T. Hasobe, H. Imahori, P. V. Kamat, T. K. Ahn, S. K. Kim, D. Kim, A. Fujimoto, T. Hirakawa, S. Fukuzumi, *J. Am. Chem. Soc.* **2005**, *127*, 1216.
112 H. Imahori, A. Fujimoto, S. Kang, H. Hotta, K. Yoshida, T. Umeyama, Y. Matano, S. Isoda, *Adv. Mater.* **2006**, *17*, 1727.
113 H. Imahori, A. Fujimoto, S. Kang, H. Hotta, K. Yoshida, T. Umeyama, Y. Matano, S. Isoda, M. Isosomppi, N. V. Tkachenko, H. Lemmetyinen, *Chem. Eur. J.* **2005**, *11*, 7265.
114 H. Imahori, K. Mitamura, T. Umeyama, K. Hosomizu, Y. Matano, K. Yoshida, S. Isoda, *Chem. Commun.* **2006**, 406.
115 H. Imahori, A. Fujimoto, S. Kang, H. Hotta, K. Yoshida, T. Umeyama, Y. Matano, S. Isoda, *Tetrahedron* **2006**, *62*, 1955.
116 H. Imahori, K. Mitamura, Y. Shibano, T. Umeyama, Y. Matano, K. Yoshida, S. Isoda, Y. Araki, O. Ito, *J. Phys. Chem. B* **2006**, *110*, 11399.
117 S. Kang, T. Umeyama, M. Ueda, Y. Matano, H. Hotta, K. Yoshida, S, Isoda, H. Imahori, *Adv. Mater.* **2006**, *18*, 2549.
118 H. Imahori, *J. Mater. Chem.* **2007**, *17*, 31.
119 N. Martín, L. Sánchez, B. IIIescas, I. Pérez, *Chem. Rev.* **1998**, *98*, 2527.
120 M. Prato, *J. Mater. Chem.* **1997**, *7*, 1097.
121 F. Diederich, M. Gómez-López, *Chem. Soc. Rev.* **1999**, *28*, 263.
122 D. M. Guldi, *Chem. Commun.* **2000**, 321.
123 D. M. Guldi, *Chem. Soc. Rev.* **2002**, *31*, 22.
124 N. Armaroli, *Photochem. Photobiol. Sci.* **2003**, *2*, 73.
125 N.-F. Nierengarten, *New J. Chem.* **2004**, *28*, 1177.
126 J. M. Lawson, A. M. Oliver, D. F. Rothenfluh, Y.-Z. An, G. A. Ellis, M. G. Ranasinghe, S. I. Khan, A. G. Franz, P. S. Ganapathi, M. J. Shephard, M. N. Paddon-Row, Y. Rubin, *J. Org. Chem.* **1996**, *61*, 5032.
127 R. M. Williams, M. Koeberg, J. M. Lawson, Y.-Z. An, Y. Rubin, M. N. Paddon-Row, J. W. Verhoeven, *J. Org. Chem.* **1996**, *61*, 5055.
128 D. Gust, T. A. Moore, A. L. Moore, *Res. Chem. Intermed.* **1997**, *23*, 621.
129 M. L. McGlashen, M. E. Blackwood, Jr., T. G. Spiro, *J. Am. Chem. Soc.* **1993**, *115*, 2074.
130 T. Kato, M. Tachiya, *Chem. Phys. Lett.* **1995**, *241*, 463.
131 G. Duskesas, S. Larsson, *Theor. Chem. Acc.* **1997**, *97*, 110.
132 S. Larsson, A. Klimkans, L. Rodriguez-Monge, G. Duskesas, *J. Mol. Struct.* **1998**, *425*, 155.
133 S. Fukuzumi, I. Nakanishi, T. Suenobu, K. M. Kadish, *J. Am. Chem. Soc.* **1999**, *121*, 3468.
134 D. M. Guldi, K.-D. Asmus, *J. Am. Chem. Soc.* **1997**, *119*, 5744.
135 S. Fukuzumi, K. Ohkubo, H. Imahori, D. M. Guldi, *Chem. Eur. J.* **2003**, *9*, 1585.
136 D. Gust, T. A. Moore, A. L. Moore, A. N. Macpherson, A. Lopez, J. M. DeGraziano, I. Gouni, E. Bittersmann, G. R. Seely, F. Gao, R. A. Nieman, X. C. Ma, L. J. Demanche, S.-C. Hung, D. K. Luttrull, S.-J. Lee, P. K. Kerrigan, *J. Am. Chem. Soc.* **1993**, *115*, 11141.
137 M. R. Wasielewski, G. L. Gains, III, G. P. Wiederrecht, W. A. Svec, M. P. Niemczyk, *J. Am. Chem. Soc.* **1993**, *115*, 10442.
138 P. Seta, E. Bienvenue, A. L. Moore, P. Mathis, R. V. Bensasson, P. A. Liddell, P. J. Pessiki, A. Joy, T. A. Moore, D. Gust, *Nature* **1985**, *316*, 653.
139 M. Fujihira, K. Nishiyama, H. Yamada, *Thin Solid Films* **1985**, *132*, 77.
140 Y. Sakata, H. Tatemitsu, E. Bienvenue, P. Seta, *Chem. Lett.* **1988**, 1625.
141 Y. Nishikata, A. Morikawa, M. Kakimoto, Y. Imai, Y. Hirata, K. Nishiyama, M. Fujihira, *J. Chem. Soc., Chem. Commun.* **1989**, 1772.
142 X. D. Wang, B. W. Zhang, J. W. Bai, Y. Cao, X. R. Xiao, J. M. Xu, *J. Phys. Chem.* **1992**, *96*, 2886.
143 K. Liang, K.-Y. Law, D. G. Whitten, *J. Phys. Chem. B* **1997**, *101*, 540.
144 G. Steinberg-Yfrach, P. A. Liddell, S.-C. Hung, A. L. Moore, D. Gust, T. A. Moore, *Nature* **1997**, *385*, 239.
145 G. Steinberg-Yfrach, J.-L. Rigaud, E. N. Durantini, A. L. Moore, D. Gust, T. A. Moore, *Nature* **1998**, *392*, 479.
146 R. F. Khairutdinov, J. K. Hurst, *Nature* **1999**, *402*, 509.
147 *Introduction to Ultrathin Organic Films*, ed. by A. Ulman, Academic Press, San Diego, **1991**.
148 A. Ulman, *Chem. Rev.* **1996**, *96*, 1533.
149 T. Kondo, T. Ito, S. Nomura, K. Uosaki, *Thin Solid Films* **1996**, *284–285*, 652.
150 K. Uosaki, T. Kondo, X.-Q. Zhang, M. Yanagida, *J. Am. Chem. Soc.* **1997**, *119*, 8367.
151 T. Kondo, M. Yanagida, S.-i. Nomura, T. Ito, K. Uosaki, *J. Electroanal. Chem.* **1997**, *438*, 121.
152 H. Imahori, H. Norieda, S. Ozawa, K. Ushida, H. Yamada, T. Azuma, K. Tamaki, Y. Sakata, *Langmuir* **1998**, *14*, 5335.
153 T. Kondo, T. Kanai, K. Iso-o, K. Uosaki, *Z. Phys. Chem.* **1999**, *212*, 23.
154 H. Imahori, T. Azuma, S. Ozawa, H. Yamada, K. Ushida, A. Ajavakom, H. Norieda, Y. Sakata, *Chem. Commun.* **1999**, 557.
155 H. Imahori, T. Azuma, A. Ajavakom, H. Norieda, H. Yamada, Y. Sakata, *J. Phys. Chem. B* **1999**, *103*, 7233.
156 H. Imahori, H. Norieda, Y. Nishimura, I. Yamazaki, K. Higuchi, N. Kato, T. Motohiro, H. Yamada, T. Tamaki, M. Arimura, Y. Sakata, *J. Phys. Chem. B* **2000**, *104*, 1253.
157 D. Hirayama, T. Yamashiro, K. Takimiya, Y. Aso, T. Otsubo, H. Norieda, H. Imahori, Y. Sakata, *Chem. Lett.* **2000**, 570.
158 M. Lahav, V. Heleg-Shabtai, J. Wasserman, E. Katz, I. Willner, H. Dürr, Y.-Z. Hu, S. H. Bossmann, *J. Am. Chem. Soc.* **2000**, *122*, 11480.
159 H. Yamada, H. Imahori, Y. Nishimura, I. Yamazaki, S. Fukuzumi, *Chem. Commun.* **2000**, 1921.
160 T. Morita, S. Kimura, S. Kobayashi, *J. Am. Chem. Soc.* **2000**, *122*, 2850.
161 H. Imahori, T. Hasobe, H. Yamada, Y. Nishimura, I. Yamazaki, S. Fukuzumi, *Langmuir* **2001**, *17*, 4925.
162 A. Ikeda, T. Hatano, S. Shinkai, T. Akiyama, S. Yamada, *J. Am. Chem. Soc.* **2001**, *123*, 4855.
163 F. B. Abdelrazzaq, R. C. Kwong, M. E. Thompson, *J. Am. Chem. Soc.* **2002**, *124*, 4796.
164 A. Nomoto, Y. Kobuke, *Chem. Commun.* **2002**, 1104.
165 D. Hirayama, K. Takimiya, Y. Aso, T. Otsubo, T. Hasobe, H. Yamada, H. Imahori, S. Fukuzumi, Y. Sakata, *J. Am. Chem. Soc.* **2002**, *124*, 532.
166 A. Ikeda, T. Hatano, T. Konishi, J.-I. Kikuchi, S. Shinkai, *Tetrahedron* **2003**, *59*, 3537.
167 E. Soto, J. C. MacDonald, C. G. F. Cooper, W. G. McGimpsey, *J. Am. Chem. Soc.* **2003**, *125*, 2838.
168 K.-S. Kim, M.-S. Kang, H. Ma, A. K.-Y. Jen, *Chem. Mater.* **2004**, *16*, 5058.
169 S. Saha, L. E. Johansson, A. H. Flood, H.-R. Tseng, J. I. Zink, J. F. Stoddart, *Small* **2005**, *1*, 87.
170 S. Saha, E. Johansson, A. H. Flood, H.-R. Tseng, J. I. Zink,

J. F. Stoddart, *Chem. Eur. J.* **2005**, *11*, 6846.
171 M. Morisue, S. Yamatsu, N. Haruta, Y. Kobuke, *Chem. Eur. J.* **2005**, *11*, 5563.
172 Y.-J. Cho, T. K. Ahn, H. Song, K. S. Kim, C. Y. Lee, W. S. Seo, K. Lee, S. K. Kim, D. Kim, J. T. Park, *J. Am. Chem. Soc.* **2005**, *127*, 2380.
173 M. Hiramoto, H. Fujiwara, M. Yokoyama, *Appl. Phys. Lett.* **1991**, *58*, 1062.
174 G. Yu, J. Gao, J. C. Hummelen, F. Wudl, A. J. Heeger, *Science* **1995**, *270*, 1789.
175 J. J. M. Halls, C. A. Walsh, N. C. Greenham, E. A. Marseglia, R. H. Friend, S. C. Moratti, A. B. Holmes, *Nature* **1995**, *376*, 498.
176 M. Granström, K. Petritsch, A. C. Arias, A. Lux, M. R. Andersson, R. H. Friend, *Nature* **1998**, *395*, 257.
177 L. S. Roman, W. Mammo, L. A. A. Pettersson, M. R. Andersson, P. Inganäs, *Adv. Mater.* **1998**, *10*, 774.
178 T. Tsuzuki, Y. Shirota, J. Rostalski, D. Meissner, *Sol. Energy Mater. Sol. Cells* **2000**, *61*, 1.
179 E. Peeters, P. A. van Hal, J. Knol, C. J. Brabec, N. S. Sariciftci, J. C. Hummelen, R. A. J. Janssen, *J. Phys. Chem. B* **2000**, *104*, 10174.
180 J.-F. Eckert, J.-F. Nicoud, J.-F. Nierengarten, S.-G. Liu, L. Echegoyen, F. Barigelletti, N. Armaroli, L. Ouali, V. Krasnikov, G. Hadziioannou, *J. Am. Chem. Soc.* **2000**, *122*, 7467.
181 S. E. Shaheen, C. J. Brabec, N. S. Sariciftci, F. Padinger, T. Fromherz, J. C. Hummelen, *Appl. Phys. Lett.* **2001**, *78*, 841.
182 L. Schmidt-Mende, A. Fechtenkötter, K. Müllen, E. Moons, R. H. Friend, J. D. MacKenzie, *Science* **2001**, *293*, 1119.
183 A. M. Ramos, M. T. Rispens, J. K. J. van Duren, J. C. Hummelen, R. A. J. Janssen, *J. Am. Chem. Soc.* **2001**, *123*, 6714.
184 C. J. Brabec, A. Cravino, G. Zerza, N. S. Sariciftci, R. Kiebooms, D. Vanderzande, J. C. Hummelen, *J. Phys. Chem. B* **2001**, *105*, 1528.
185 D. L. Vangeneugden, D. J. M. Vanderzande, J. Salbeck, P. A. van Hal, R. A. J. Janssen, J. C. Hummelen, C. J. Brabec, S. E. Shaheen, N. S. Sariciftci, *J. Phys. Chem. B* **2001**, *105*, 11106.
186 F. Zhang, M. Svensson, M. R. Andersson, M. Maggini, S. Bucella, E. Menna, O. Inganäs, *Adv. Mater.* **2001**, *13*, 1871.
187 W. U. Huynh, J. J. Dittmer, A. P. Alivisatos, *Science* **2002**, *295*, 2425.
188 D. M. Guldi, C. Luo, A. Swartz, R. Gómez, J. L. Segura, N. Martín, C. Brabec, N. S. Sariciftci, *J. Org. Chem.* **2002**, *67*, 1141.
189 F. Padinger, R. S. Rittberger, N. S. Sariciftci, *Adv. Funct. Mater.* **2003**, *13*, 85.
190 M. M. Wienk, J. M. Kroon, W. J. H. Verhees, J. Knol, J. C. Hummelen, P. A. Van Hal, R. A. J. Janssen, *Angew. Chem., Ind. Ed.* **2003**, *42*, 3371.
191 J. Xue, S. Uchida, B. P. Rand, S. R. Forrest, *Appl. Phys. Lett.* **2004**, *84*, 3013.
192 W. Ma, C. Yang, X. Gong, K. Lee, A. J. Heeger, *Adv. Funct. Mater.* **2005**, *15*, 1617.
193 J. Xue, B. P. Rand, S. Uchida, S. R. Forrest, *Adv. Mater.* **2005**, *17*, 66.
194 H. Hoppe, N. S. Sariciftci, *J. Mater. Chem.* **2006**, *16*, 45.
195 B. O'Regan, M. Grätzel, *Nature* **1991**, *353*, 737.
196 A. Hagfeldt, M. Grätzel, *Acc. Chem. Res.* **2000**, *33*, 269.
197 M. Grätzel, *Chem. Lett.* **2005**, *34*, 8.
198 P. V. Kamat, S. Barazzouk, K. G. Thomas, S. Hotchandani, *J. Phys. Chem. B* **2000**, *104*, 4014.
199 H. Imahori, M. Arimura, T. Hanada, Y. Nishimura, I. Yamazaki, Y. Sakata, S. Fukuzumi, *J. Am. Chem. Soc.* **2001**, *123*, 335.
200 S. Fukuzumi, Y. Endo, Y. Kashiwagi, Y. Araki, O. Ito, H. Imahori, *J. Phys. Chem. B* **2003**, *107*, 11979.
201 H. Imahori, Y. Kashiwagi, T. Hanada, Y. Endo, Y. Nishimura, I. Yamazaki, S. Fukuzumi, *J. Mater. Chem.* **2003**, *13*, 2890.
202 H. Imahori, Y. Kashiwagi, Y. Endo, T. Hanada, Y. Nishimura, I. Yamazaki, Y. Araki, O. Ito, S. Fukuzumi, *Langmuir* **2004**, *20*, 73.
203 T. Hasobe, P. V. Kamat, V. Troiani, N. Solladié, T. K. Ahn, S. K. Kim, D. Kim, A. Kongkanand, S. Kuwabata, S. Fukuzumi, *J. Phys. Chem. B* **2005**, *109*, 19.
204 T. Hasobe, S. Hattori, P. V. Kamat, S. Fukuzumi, *Tetrahedron* **2006**, *62*, 1937.

Hiroshi Imahori was born in Kyoto, Japan in 1961. He completed his doctorate in organic chemistry at Kyoto University. In 1990–1992, he was a post-doctoral fellow at the Salk Institute for Biological Studies, U.S.A. In 1992, he became an Assistant Professor at ISIR, Osaka University. In 1999, he moved to the Graduate School of Engineering, Osaka University, as an Associate Professor. Since 2002, he has been a Professor of Chemistry, Graduate School of Engineering, Kyoto University. During 2001–2005, he was a project leader of a PRESTO project of Japan Science and Technology Agency (JST). He received a Young Investigator Award from the Society of Porphyrins and Phthalocyanines (2002), the Japanese Photochemistry Association Prize (2004), JSPS prize (2006), and the CSJ Award for Creative Work (2006). His current interests involve artificial photosynthesis, organic solar cells, photofunctional materials, self-assembly, and porphyrin–fullerene chemistry. To date, Hiroshi Imahori has written more than 140 original papers.